Insight into Nucleation of Microtubules to Realize Novel Drug Targets

BY

CHARU SURI
Enrollment No. 116503

SYNOPSIS
OF THE THESIS SUBMITTED IN FULFILLMENT OF THE REQUIREMENTS FOR

THE DEGREE OF DOCTOR OF PHILOSOPHY
IN
BIOINFORMATICS

UNDER THE GUIDANCE OF
DR. PRADEEP KUMAR NAIK

DEPARTMENT OF BIOTECHNOLOGY & BIOINFORMATICS
JAYPEE UNIVERSITY OF INFORMATION TECHNOLOGY
WAKNAGHAT, SOLAN – 173 234, H.P., INDIA

SEPTEMBER 2014

Insight into Nucleation of Microtubules to Realize Novel Drug Targets

CHARU SURI

INTRODUCTION

Microtubules are highly dynamic cytosketal polymers that are built up of heterodimers of α- and β-tubulin proteins that self assembles in a head to tail fashion to make long protofilaments. Generally, thirteen of theses protofilaments then assemble laterally to form a sheet which then folds into a hollow cylinder to form microtubule. The linear arrangement of α/β tubulin also gives a polarity to resulting microtubules that display dynamic instability in that they continually undergo lengthening and shortening at both ends—more rapidly at one end (known as plus end) than the other slower end (known as minus end). Microtubules are key component of mitotic spindle apparatus that is necessary for the alignment and subsequent segregation of duplicated chromosomes into daughter cells during cell division. They play a vital role in many other cellular functions including cell polarity, cell motility, transport of intracellular organelles, and maintenance of the overall cellular morphology. Such a myriad of roles calls for a very rapid reorganization of microtubules.

Microtubule assemblies, obtained *in vitro* from purified tubulin, differ from microtubule assemblies *in vivo* [1]. *In vitro*, disassembly is energetically favoured over the assembly process until a critically large oligomer is formed [2]. Cells overcome this slow initial phase of the assembly process by providing specific nucleation sites called microtubule organization centers (MTOC), which in most animal cells is a centrosome [3]. The initiation of microtubule assembly within cells is guided by a cone shaped multi-protein complex containing another member of tubulin family, γ-tubulin and at least five other γ-tubulin-complex proteins (GCPs) i.e., GCP2, GCP3, GCP4, GCP5, and GCP6. The rim of this cone-shaped complex is a ring of γ-tubulin molecules that directly interacts via one of its longitudinal interfaces with the GCP2, GCP3 or GCP4 and via its other interface with the α/β tubulin dimers (Figure 1). Experimental methods have shown that γ-tubulin interacts with the minus end of the microtubules to facilitate microtubule nucleation [4]. γ-tubulin is present at the MTOC in a complex called γ-tubulin small complex (γTuSC), which is composed of two copies of γ-tubulin and one copy each of gamma complex protein 2 (GCP2) and gamma complex protein 3 (GCP3) [5] (Figure 2). Multiple copies of γTuSC along with GCP4, GCP5 and GCP6 associate together to form γ-tubulin ring complex (γTuRC) in eukaryotes as a unit for microtubule assembly nucleation [6]. Among the multiple proposed hypothetical models, the 'template model' is widely accepted that presents a ring of γ-tubulin on top of the γTuRC as the template.

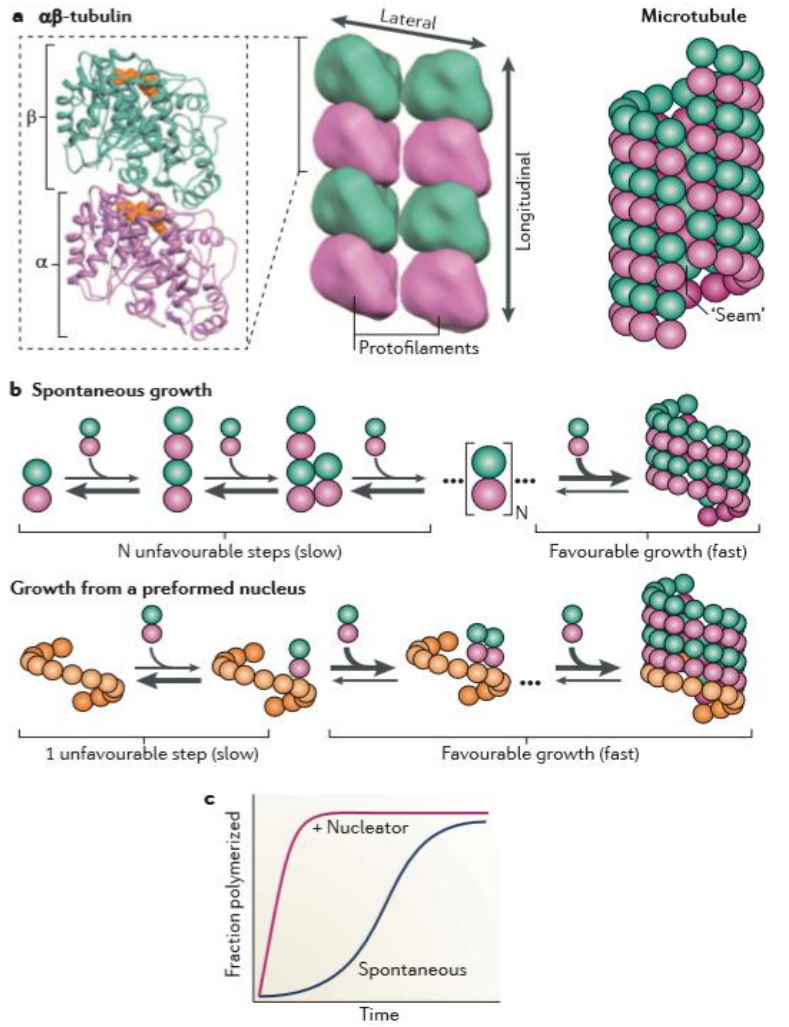

Figure 1: Microtubule assembly. a: The α/β tubulin heterodimer is the fundamental repeating subunit of microtubules. When bound to GTP (shown in orange in the left panel), heterodimers come together through two types of contacts. In 13 protofilament microtubules, a 'seam' is formed as a result of lateral α-tubulin and β-tubulin interactions.

b: Spontaneous microtubule growth is relatively slow through unstable early assembly intermediates phase, while rapid in elongation phase.

c: In bulk assembly assays, the presence of a nucleator causes rapid microtubule polymerization, bypassing the lag phase observed during spontaneous growth. (Kollman *et al*., 2011) [7].

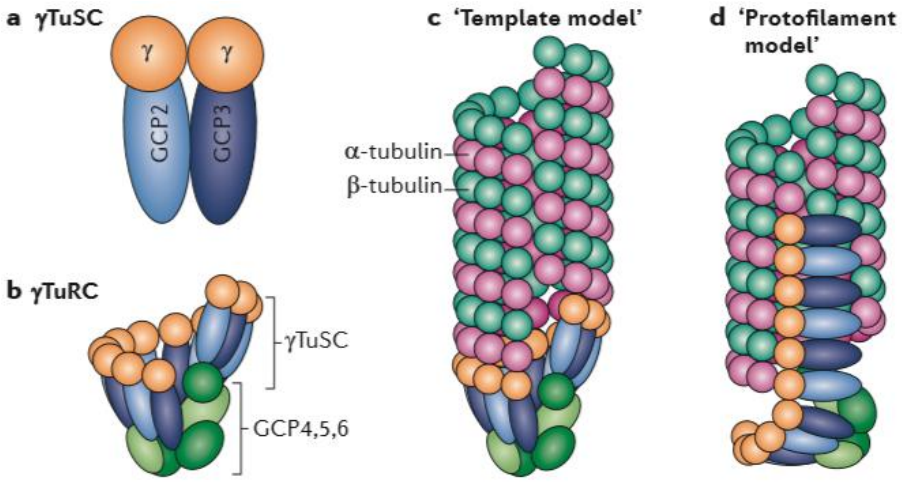

Figure 2: γ-tubulin ring complex. **a**: The γTuSC has two copies of γ-tubulin and one each of γ-tubulin complex protein 2 (GCP2) and GCP3. **b**: In many eukaryotes, multiple γTuSCs assemble with GCP4, GCP5 and GCP6 into the γ-tubulin ring complex (γTuRC). **c**:The most widely accepted model for the mechanism of γTuRC-based nucleation, the 'template model', suggests that the γTuRC acts as a template, presenting a ring of γ-tubulins that make longitudinal contacts with α- and β- tubulin (αβ-tubulin). **d**: The 'protofilament model' suggests a γ-tubulin protofilament, which would nucleate through lateral contacts with αβ-tubulin (Kollman *et al*., 2011 [7]).

In this model each γ-tubulin subunit interacts longitudinally, via one of its interface, with the α/β-tubulin unit, via the other longitudinal interface with GCP2, GCP3 and GCP4 and laterally with another γ-tubulin unit. Nevertheless the mode and mechanism of these interactions are not clearly described.

γ-tubulin is a small globular protein, homologous to α/β tubulins and is most noticeably localized at the MTOC in eukaryotes [8-14]. However, unlike α- and β-tubulins, γ-tubulin does not polymerize into the microtubule lattice, but is instead recruited to the microtubule organizing centers [12,13]. γ-tubulin is indispensible for the microtubule spindle function in mitosis and its absence causes cell death [8, 12]. Recent studies have also indicated that γ-tubulin might also have a role in the regulation of microtubule dynamics at the plus end [15]. Additionally, although tubulins (α/β) are abundant proteins constituting roughly 2.5% of the total protein in a cell, γ-tubulin makes up for less than 1% of the total tubulin content of the cell [10]. Higher expression of γ-tubulin has been associated with pre-invasive lesions and carcinomas of the breast and prostate cancer, thyroid carcinomas and glioblastoma multiforme [16-21]. Therefore, γ-tubulin has a clearly high potential of proving to be an excellent drug target for cancer therapy. Therefore, there is immense interest in developing promising leads that will be useful to design γ-tubulin interacting agents. For example, using a fragment based approach combined with biophysical screening of several small molecules; Cala *et al*. in 2013, identified potential γ-tubulin interacting agents preferably at the γ-tubulin-GCP4 binding interface [22].

In this study, we therefore strive to elucidate the molecular basis of interaction of γ-tubulin with another γ-tubulin unit, GCP4 and α/β-tubulin using molecular modelling and molecular dynamics simulations. We elucidated the protein-protein interactions of γ-tubulin with adjacent γ-tubulin, GCP4 and α/β-tubulin using molecular dynamics simulations followed by MMPB/GB-SA and *in silico* alanine scanning mutation analyses. Findings were further verified using computational and experimental alanine scanning mutation analyses. Furthermore, we attempted to explore the interaction interfaces between the adjacent γ-γ tubulin subunits and γ-tubulin-GCP4 as novel potent target for development of chemotherapeutic drugs. In the endeavour to identify chemical leads that might interact with γ-tubulin and disrupt its function; we have evaluated the binding affinity of noscapine and its derivatives onto the cavity close to γ-γ-tubulin interface as well as the γ-tubulin-GCP4 interface. All noscapinoids displayed stable interaction throughout the simulation. This offers a novel chemical scaffolds for γ-tubulin binding drugs near γ- γ-tubulin and γ-tubulin-GCP4 interface.

Objectives:

1. **To elucidate the γ-γ tubulin lateral interactions of the γ-complex ring:** We have utilised computational methods to determine the extent of the lateral atomic interaction between two adjacent γ-tubulins. Further, the predicted result was verified using computational and experimental mutagenesis.

2. **To identify chemical leads that interfere with γ-γ tubulin lateral interactions of the γ-complex ring and disrupt its function:** Towards this end we evaluated the binding affinity of noscapine and its derivatives at the interface of γ-γ tubulin. This offered a novel chemical scaffold for γ-tubulin binding drugs.

3. **To understand atomic interactions between γ-tubulin and GCP4 using molecular modelling calculations:** Towards this end we have performed a long run of MD simulations of γ-tubulin-GCP4 complex to stabilize the system followed by calculating the binding free energy between binding of GCP4 with γ-tubulin using both MM-PBSA and MM-GBSA computational methods. Further the amino acids crucial for the interaction of γ-tubulin with GCP4 were identified by computational alanine-scanning mutagenesis.

4. **To identify chemical leads that might interact at the interface between γ-tubulin and GCP4:** We evaluated the binding affinity of noscapine and its derivatives. To ascertain the possibility of binding of noscapinoids at the interface of γ-tubulin and GCP4, we compared their binding affinity against experimentally proven compounds that bind at the interface region.

5. **To elucidate the interaction of γ tubulin with α/β tubulin heterodimers:** To achieve this goal we first established a complex between γ-tubulin and α/β tubulin using protein-protein docking, followed by long run of MD simulation and calculation of free energy of binding of γ-tubulin onto α/β tubulin using MM-GBSA and MM-PBSA computational methods. The predicted site of interface between γ-tubulin and α/β tubulin was evaluated using computational alanine scanning mutation. Further the predicted result was correlated with the experimental data to validate the interactions between γ-tubulin and α/β tubulin heterodimers.

CHAPTER 1 - Insight into γ-γ tubulin lateral interactions of the γ-complex ring.

According to the template model, γ-tubulins associate laterally with each other in the γTuRC. In this study we explored the molecular basis of lateral interaction between the adjacent γ-tubulins using molecular modelling and molecular dynamics computational approaches. We performed MM-PBSA and MM-GBSA analyses to predict theoretical binding affinity between the two γ tubulin units. We also calculated energy contribution of each amino acid of γ tubulin to the stability of the γ-γ tubulin homodimer to identify hot spot amino acids. These hot spot amino acids were then verified using experimental and computational alanine scanning mutagenesis.

Materials and Methods

Molecular system

The initial co-ordinates of γ-tubulin homodimer (PDB_ID:3CB2, Res: 2.3Å) was obtained from Protein DataBank (PDB) [23]. During the initial screening of the γ- tubulin dimer many errors such as missing residues and missing side chains were observed. These errors were fixed based on homology modelling technique using multiple templates in Prime (version 3.0, Schrödinger). The modelled structure was subjected to energy minimization in Macromodel (version 9.9, Schrödinger) using Polak-Ribiere Conjugate Gradient (PRCG) algorithm and OPLS 2005 force field with a gradient of 0.001 kcal/mol and 1000 steps of iterations.

To further refine the structure, a small run of all atom Molecular Dynamics (MD) simulations was carried out for 1000 ps with a time step of 2 fs on the modelled structure using Gromacs package (Version 4.5.4) [24]. The simulations were set up with Gromos96 force field, in a dodecahedron solvation box at a distance of 12Å from the periphery of the protein. Prior to the 1000 ps MD Simulation the molecular system was neutralized with 9 Na+ ions, energy relaxed using steepest descent algorithm for 1000 steps and then equilibrated for 100 ps of MD run. An average structure was generated using the last 200 frames from the total of 1000 frames generated during MD simulation. The γ-dimer was than reconstituted by substituting the coordinates from the refined structure of 'A' chain onto the original crystal structure, preserving the original geometry and orientation (Figure I). Furthermore, the γ-γ dimer obtained was energy minimized. The overall quality of the reconstituted γ-γ homodimer was determined using PROCHECK [25, 26], ERRAT [27] and VERIFY3D [28] (Figure 3). In order to study the molecular interactions in γ-γ complex, the dimer structure reconstituted above was simulated using Molecular Dynamics in Amber 11.0 and Ambertools 1.5 [29, 30].

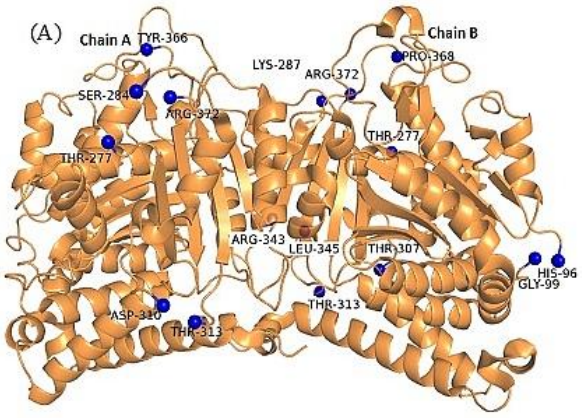

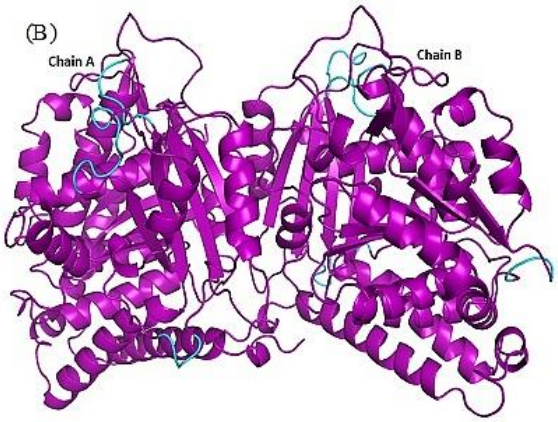

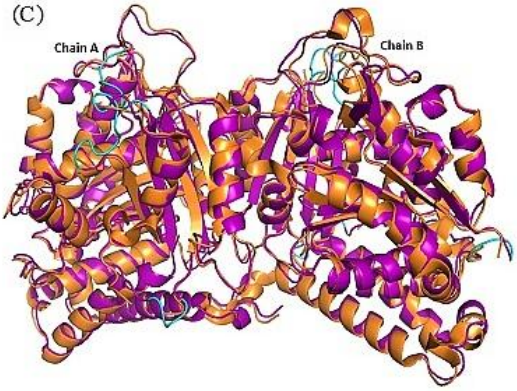

(D)

	Crystal structure of γ-γ dimer (3CB2)	Refined structure of γ-γ dimer
Verify3D	88.91%	91.93%
Errat	96	91.44
Ramachandran plot:		
Allowed region	99.7%	99.7%
Disallowed region	0.3%	0.3%

Figure 3: Crystal structure of γ-γ dimer and its refined structure. Panel 'A' shows the crystal structure of γ-γ dimer (PDB ID: 3CB2) with gaps. Gap flanking residues are shown as blue spheres. Panel 'B' shows the refined structure of γ-γ dimer. A total of 14 missing residues were added and these can be seen in cyan colour. Panel 'C' shows the refined structure of γ-γ dimer (purple) superimposed over the initial crystal structure of γ-γ dimer obtained from 3CB2 (orange); calculated RMSD was 0.73Å. Panel 'D' gives the structure quality parameters of both the wild type and refined structure of γ-γ dimer.

Molecular Dynamic simulation

Since we intended to understand the molecular interaction between adjacent γ-tubulins, we MD simulated the dimer using Amber 11.0 and Ambertools 1.5 [32,33]. Tleap program implemented in Amber 11 was used to assign parameters from FF99SB force field, neutralize the system, solvate the system using TIP3P model and finaly generated the toplogy and co-ordinate files [34-36]. Prior to molecular dynamics simulation, both the dimeric complexes were relaxed to remove bad contacts. Each complex was subjected to three consecutive rounds of 1000 step minimization employing 500 steps of steepest descent followed by 500 steps of conjugate gradient methods. For the first and second rounds only water molecules were relaxed while the protein was held fixed using force constants of 10 and 2 kcal mol^{-1} $Å^{-2}$ respectively. In the third round the entire system was allowed to relax without any restraint. The fully relaxed structure was then heated to 300 K in 100 ps. The system was subjected to density equilibration over 100 ps followed by 500 ps of constant pressure equilibration at 300 K and 1 atm pressure with a force constant of 2 kcal mol^{-1} $Å^{-2}$. A 10 ns MD simulation was carried out on the equilibrated system using Particle Mesh Ewald Molecular Dynamics method using the time step of 2 fs [37, 38]. Through out the simulation

the Langevin thermostat was used to regulate the temperature and the bond lengths involving hydrogen bonds were constrained using SHAKE algorithm [39]. MD was carried out in an NPT ensemble using a Berendsen barostat [40] with a target pressure of 1 atm. The structures were recoreded every 1 ps resulting in a trajectory with 10,000 frames.

Theoretical binding affinity calculation

The calculation of binding free energy in solvation, between the γ-tubulin units in the dimer was determined using the conventional MM-PBSA and MM-GBSA approaches described in Amber 11 [31,32]. Out of the total 5000 frames obtained during MD simulation 250 frames were extracted every 20 ps from last 5 ns of the MD trajectory for calculation of the ensemble average of binding free energy. The binding free energy was calculated considering each molecular species (complex, receptor and ligand) and the binding free energy was calculated as follows.

$$\Delta G_{bind} = \Delta G_{complex} - [\Delta G_{protein} + \Delta G_{lig}]$$

Energy decomposition and computational alanine scanning

Binding free-energy contributions of each residue at the protein-protein interaction interface were calculated using the GB model, implemented in Amber11, on the basis of 250 snapshots extracted every 20 ps from the last 5 ns of MD simulation trajectory [43,44]. On the basis of individual contributions to the binding free energy of the complex, those amino acids contributed more significantly to the binding free energy (contribution > 2.0 kcal/mol) were identified as the hotspot amino acids [33-35]. These hotspot amino acids were believed to contribute most to the stability of complex and are significant for the γ-γ tubulin interaction.

To further study the energy contribution of these amino acids in the interaction of γ-γ tubulin, computational alanine scanning was performed. In this method an amino acid of interest is replaced with alanine and absolute binding free energy is recalculated. In our study the hotspot amino acids were mutated to alanine and binding free energies were calculated for the resulting mutated system using the MM-GBSA approach on the 250 snapshots extracted every 20 ps from the last 5 ns of MD simulation. Finally, the difference in the binding free energies of the mutant and wild type, $\Delta\Delta G_{bind}$, was computed as follows:

$$\Delta\Delta G_{bind} = \Delta G_{bind}\ [\text{Mutant}] - \Delta G_{bind}\ [\text{Wild Type}]$$

Positive values of $\Delta\Delta G_{bind}$ indicate the favourable contribution while negative values indicate unfavorable contributions.

Experimental alanine scanning mutation and phenotypes

pALTER-EX1 vector (Promega, Madison, WI) was used to subclone *TUBG1* cDNA into the *NdeI* site downstream from the SP6 promoter to create pTWH101 as described by Hendrickson *et al*. [36]. Based on our findings from the molecular modelling methods, a stretch of five polar amino acids (Arg339, Arg341, Glu342, Arg343 and Lys344) that contributed significantly to the lateral γ-γ tubulin interactions was identified. These amino acids were mutated to alanine by oligonucleotide-directed mutagenesis using pTWH101 as the template. pALTER-EX1 contains a tetracycline resistance gene and an inactivated ampicillin resistance gene.

The yeast expression plasmids were constructed by sub cloning each of the *tubg1* alleles into pREP1 at the *NdeI* site downstream of the *nmt1+* promoter [37, 38]. Wild type cells were transformed with either one of the *tubg1*-pREP1 plasmids or the control *TUBG1*-pREP1 and grown in minimal media supplemented with adenine, histidine and uracil. Transformants were screened at 18 and 36 °C to identify conditional mutants in the presence of endogenous γ-tubulin. The strains were maintained at 30 and 26 °C, respectively. A diploid strain, NC377 [39,11], bearing one endogenous wild-type copy of *S. pombe* γ-tubulin, *gtb1+* and one disrupted copy, *gtb1::ura4+*, was also transformed with the mutant plasmids. The resulting yeast transformants were randomly sporulated and selected for *ura+, leu+*, and the spores were tested for conditional growth.

Results

The corrected structure of γ-tubulin homodimer was simulated for 10 ns (Figure 4 and Figure 5). The molecular interaction and binding free energy between γ-γ tubulin dimer was calculated based on MM-PBSA and MM-GBSA of the MD trajectories. Both the methods indicated very robust interactions between the two γ-tubulin subunits (Table 1). The ensemble average of binding free energy using MM-PBSA and MM-GBSA was determined as -107.76 kcal/mol and -87.02 kcal/mol (Table 1).

To further understand the γ-γ interactions at the atomic level, binding free energy contributions were determined for each residue in the γ-γ complex using the MM-GBSA method (Table 2). The residues having a contribution of more than 2 kcal/mol to the binding affinity were designated as hotspot amino acids and they were proposed to contribute most to the stability of the γ-γ complex. As an example Asp252, Met249, His334 of chain ‘A’ and Arg341, Met249, Asp252 of chain ‘B’ make very high free energy contributions > 4 kcal/mol hence, making considerably large contribution to the overall binding free energy of the complex. In addition to these residues, seven more residues of chain ‘A’ (Arg341, Arg265, Trp446, Ile 444, Tyr443, Pro353, Asn250) and nine amino acid residues of chain

'B' (Arg265, Hie334, Tyr443, Gln357, Lys164, Pro353, Val358, Ile444, Trp446) show high energy contribution > 2 kcal/mol to the binding affinity (Table 2).

Significantly, all the hotspot amino acids were observed to lie at the γ-γ complex interface (Figure 6). Also, we found that the non-polar energy component dominated the polar energy component for all hotspot amino acids (Figure 7).

Table 1: Ensemble average of binding free energy (kcal/mol) of γ-γ tubulin complex calculated using the MM-GBSA and MM-PBSA methods in Amber

Contribution	γ-γ Complex	Mutant γ-γ complex
ΔE_{int}	0.00	0.00
ΔE_{vdw}	-158.10	-155.06
ΔE_{ele}	-676.57	410.33
ΔE_{gas}	-834.67	255.27
ΔG_{sol-np}	-18.70	-17.68
ΔG_{PB}	745.61	-324.61
$\Delta G_{solv, PB}$	726.91	-342.28
$\Delta G_{ele, PB}$	69.04	85.72
$H_{tot, PB}$	-107.76	-87.02
ΔG_{GB}	770.11	-316.08
$\Delta G_{solv, GB}$	749.15	-335.44
$\Delta G_{ele, GB}$	93.55	94.25
$H_{tot, GB}$	-85.52	-80.17

Table 2. Decomposition of calculated ΔGbind, GB (kcal/mol) on per residue basis into van der Waals, electrostatic, polar solvation and non-polar solvation energy components

	Residue	$\Delta E_{i,vdw}$	$\Delta E_{i,ele}$	$\Delta G_{i,sol\ GB}$	$\Delta G_{i,sol-np}$	$\Delta H_{i,tot,GB}$
Chain A	MET249	-6.93	-4.61	8.20	-1.19	-4.53
	ASN250	-4.80	-12.12	15.63	-0.83	-2.11
	ASP252	-0.50	-40.48	35.85	-0.31	-5.45
	ARG265	-0.34	-66.03	62.85	-0.27	-3.80
	HIE334	-4.92	1.26	0.21	-0.75	-4.20
	ARG341	-2.91	-101.40	101.24	-0.80	-3.87
	PRO353	-2.39	-2.60	3.12	-0.50	-2.38
	TYR443	-3.44	-2.16	3.48	-0.36	-2.48
	ILE 444	-3.11	-2.51	2.51	-0.47	-3.58
	TRP 446	-6.72	49.44	-45.05	-1.28	-3.61
Chain B	LYS164	-0.07	5.71	-7.90	-0.14	-2.40
	MET249	-6.45	-3.78	6.07	-1.18	-5.33
	ASP252	-0.66	-24.97	21.49	-0.11	-4.25
	ARG265	-0.51	-67.09	64.34	-0.28	-3.54
	HIE334	-4.39	-3.34	5.51	-0.72	-2.93
	ARG341	-1.24	-102.51	98.15	-0.63	-6.23
	PRO353	-2.33	-2.75	3.23	-0.49	-2.33
	GLN357	-1.63	-6.28	5.65	-0.25	-2.51
	VAL358	-2.08	-2.73	2.78	-0.22	-2.24
	TYR443	-3.61	-2.14	3.53	-0.40	-2.62
	ILE 444	-2.89	-2.34	2.42	-0.45	-3.27
	TRP446	-6.94	49.51	-45.12	-1.34	-3.88

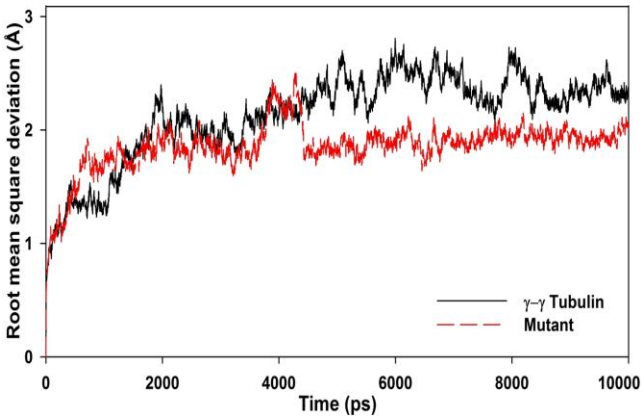

Figure 4: Root mean square deviation of γ-γ tubulin complex and mutant complex with respect to time over 10,000 picoseconds

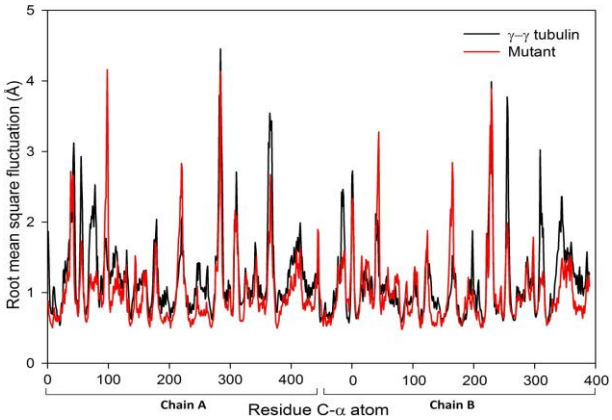

Figure 5: Root mean square fluctuations of residue Cα atom over 10,000 picosecond.

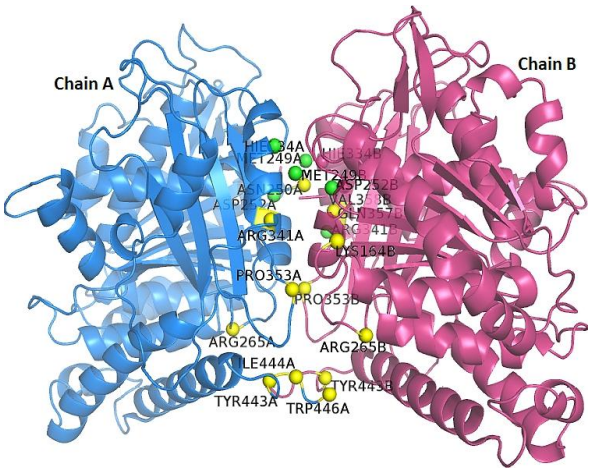

Figure 6: Hot spot amino acids to the stability of the γ-γ tubulin dimer calculated using the MM-GBSA method. C-α atoms of amino acid residues contributing > 4kcal/mol are marked green spheres while those with a contribution of 2-4 kcal/mol are marked yellow.

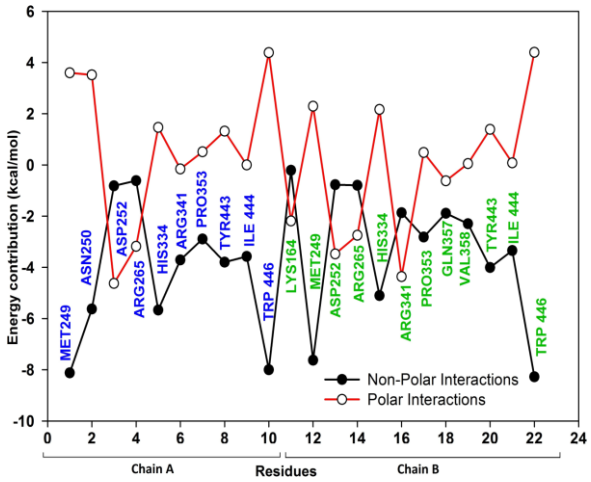

Figure 7: The polar and the non polar contributions of residues of chain A (labelled blue) and chain B (labelled green) in the γ-γ tubulin dimer calculated using MM-GBSA method.

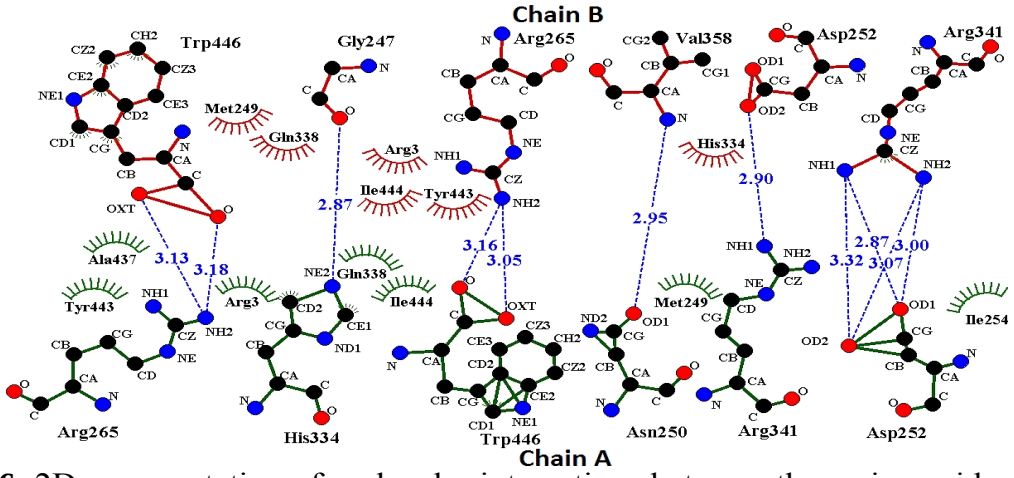

Figure 1.6: 2D representation of molecular interactions between the amino acids of the two units of γ-γ tubulin (chain 'A' and chain 'B'). Hydrogen bonding residues are shown in green and red for chain A and chain B, respectively. The Dashed lines denote hydrogen bonds, and numbers indicate hydrogen bond lengths in Å. Hydrophobic interactions are shown as arcs with radial spokes. The figures was made using Dimplot.

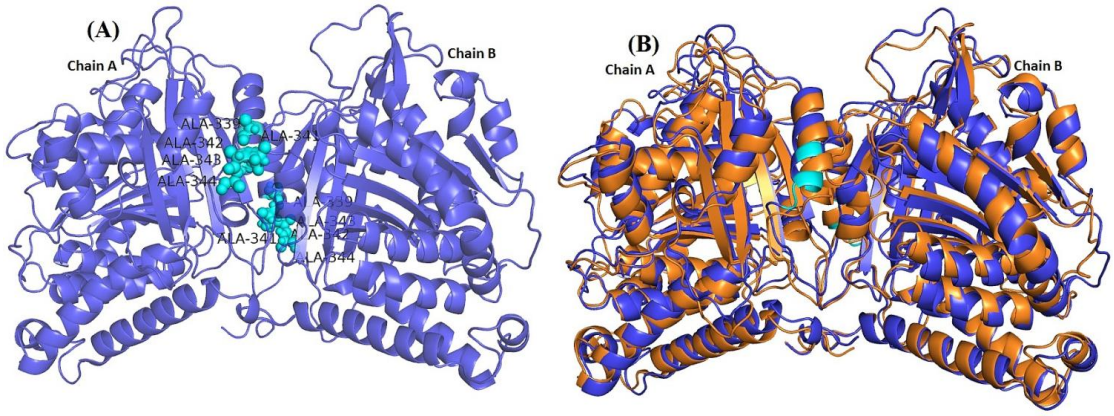

Figure 8. Mutant structure of γ-γ dimer. Panel 'A' shows the mutant structure of γ-γ dimer along with the residues mutated to alanine in cyan colour spheres. Panel 'B' shows the mutated structure of γ-tubulin dimer obtained after 10 ns MD simulation in Amber (blue) superimposed over the structure of wild type γ-tubulin dimer (Orange) obtained after 10 ns MD simulations in amber. Calculated RMSD was 1.75 Å.

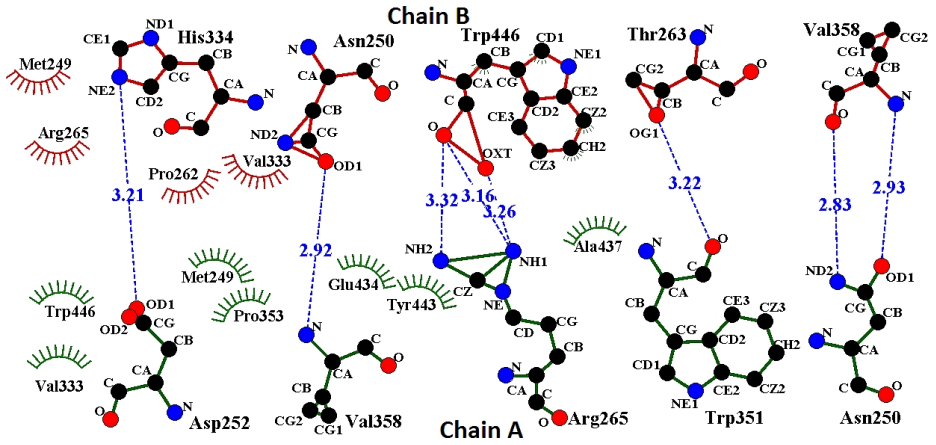

Figure 9: 2D representation of molecular interactions between the amino acids of the two mutated units of γ-γ tubulin (chain 'A' and chain 'B'). Hydrogen bonding residues are shown in green and red for chain A and chain B, respectively. The Dashed lines denote hydrogen bonds, and numbers indicate hydrogen bond lengths in Å. Hydrophobic interactions are shown as arcs with radial spokes.

Table 3: Computational Alanine scanning results for hotspot residues, for which free energy contribution was high (> 4 kcal/mol), determined using MM-PBSA and MM-GBSA method, implemented in Amber.

	Hotspot Residues	$\Delta\Delta G_{GB}$ (kcal/mol)	$\Delta\Delta G_{PB}$ (kcal/mol)
Chain A	MET249	6.43	6.15
	ASN250	4.67	5.67
	ASP252	17.49	25.00
	ARG265	6.72	7.22
	HIE334	7.52	4.80
	ARG341	8.07	11.80
	PRO353	1.72	1.70
	TYR443	3.32	1.26
	ILE 444	3.11	1.39
	TRP 446	2.9	1.42
Chain B	LYS164	1.16	1.20
	MET249	6.75	5.74
	ASP252	10.92	29.76
	ARG265	6.52	7.07
	HIE334	3.01	1.16
	ARG341	13.37	16.59
	PRO353	1.70	1.78
	GLN357	2.86	3.15
	VAL358	1.28	2.15
	TYR443	3.70	2.29
	ILE 444	2.94	1.24
	TRP446	2.8	1.2

Conclusion

In this study, the molecular basis of interaction between two lateral γ-tubulin units were elucidated by making extensive use of molecular mechanics and molecular dynamics techniques. A refined structure of γ-γ tubulin homodimer was obtained based on the initial co-ordinates from the PDB (PDB_ID:3CB2, Res: 2.3Å). The refined structure was MD simulated to obtain a 10 ns trajectory that was utilized to perform MM-PBSA/GBSA calculations and binding free-energy decomposition analyses in order to characterize interactions between two γ-tubulin units. MM-PBSA and MM-GBSA calculations revealed highly favourable non-polar component. Although some columbic contribution were found to be favourable and probably played a crucial role in the binding site recognition, the overall polar contribution was less significant to the overall binding free energy due to penalty imposed by very large desolvation energy component. Therefore, the non-polar component was considered as the driver of the molecular interactions between γ-γ tubulin. Also, on the basis of per residue free energy decomposition a total of twenty two hot spot amino acids were identified which were found to contribute highly (> 2kcal/mol) to the binding affinity between the two γ-tubulins. Computational alanine scanning was carried out

for six hotspot amino acids with high energy contribution (>4 kcal/mol) resulted in a drop of at least 4.8 kcal/mol for each hotspot amino acid (Table 3). On the basis of these findings, a mutant structure of γ-γ tubulin homodimer was obtained after mutating a stretch of five polar amino acids (Arg339, Arg341, Glu342, Arg343 and Lys344) to alanine (Figure 8). The results from MM-PBSA and MM-GBSA showed a significant drop in the binding affinity between γ-γ tubulin interactions. To test whether these mutant proteins can support life, experimental alanine scanning mutagenesis was performed and the cDNA encoding the mutant and the endogenous fission yeast γ-tubulin (*gtb1*) gene was replaced with the mutant γ-tubulin gene (*TUBG1*) in haploid cells. We found that the γ-γ tubulin mutant (*gtb1*-/alanine-TUBG1) that was predicted to disrupt interactions was unable to support growth in the absence of endogenous $gtb1^{+}$ (referred to as recessive lethal). These findings further reiterated that the hotspot amino acids identified using computational methods indeed play crucial essential role in γ-γ tubulin interactions, and when the key residues were mutated they could not support yeast cell division and growth. The observed phenotypes thus correlate well with our computational predictions of important residues for γ-tubulin interactions.

CHAPTER 2 – Molecular interactions of noscapinoids at the interface of γ-γ tubulin dimmer.

In the endeavour to explore if small ligands could bind at the interface and disrupt the γ-γ tubulin lateral interactions, we studied probable binding interaction of noscapinoids (noscapine, amino-noscapine and bromo-noscapine) with γ-tubulin homodimer. In this direction, we first prepared the structure of the γ-tubulin homodimer and ligands. We then performed molecular docking to obtain the protein –ligand complexes, which were then simulated in Amber 11 for 10 ns and then predicted the binding affinity using the MM-PBSA and MM-GBSA methods.

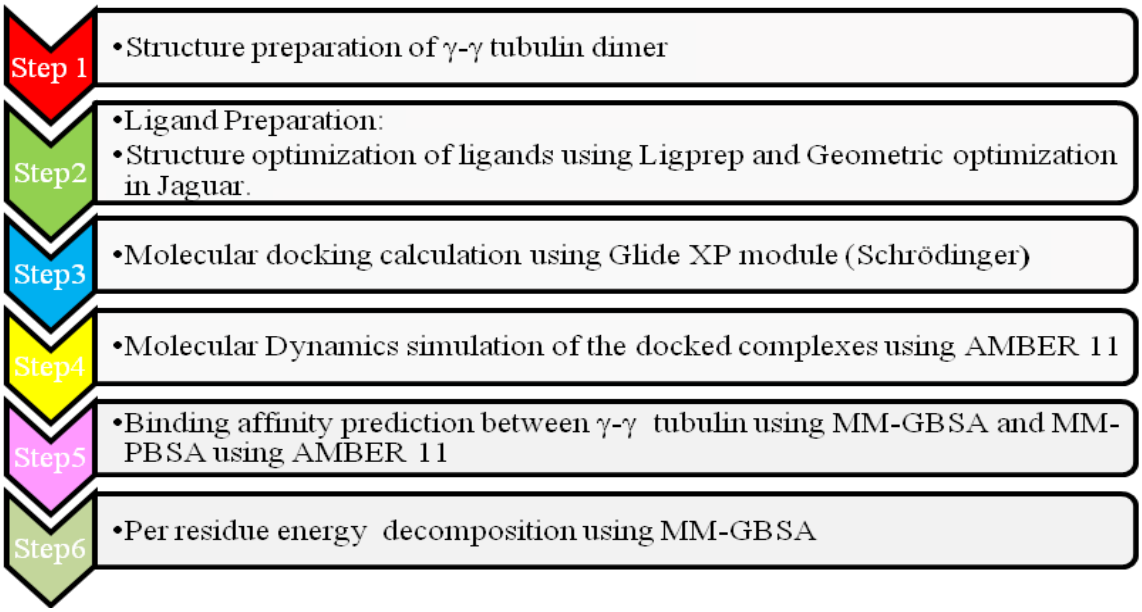

Figure 10: Schematic representaion of methodology

Materials and Methods

Protein structure preparation

In order to study the molecular interaction of noscapinoids at the binding interface of γ-γ tubulin, the structure of γ-tubulin dimer was first prepared as described in chapter 1.

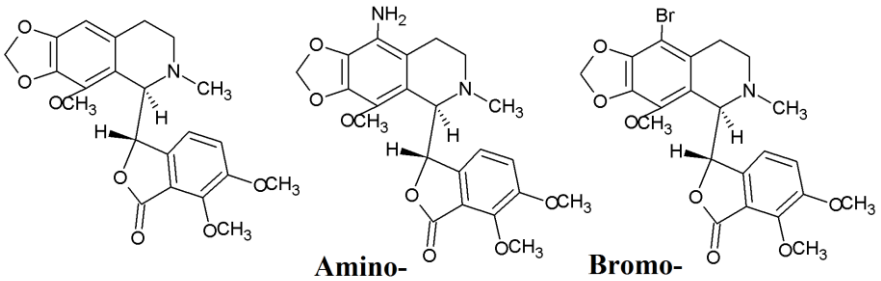

Figure 11: Molecular structure Noscapine (1), Amino-noscapine (2), Bromo-noscapine (3)

Ligand preparation

The molecular structure of the lead molecule, noscapine and two of its derivatives such as amino-noscapine and bromo-noscapine **1-3** (Figure 11) were built using molecular builder of

Maestro (version 8.5, Schrodinger LLC). All these structures were energy minimized *in-vacuo* using Impact (version 5.6, Schrodinger, LLC). Appropriate bond orders were assigned to each structure using Ligprep (version 2.4, Schrodinger LLC) and initial optimization was performed on each structure by employing OPLS 2005 force field using default setting. Furthermore, geometrical optimization of these ligands was performed in Jaguar (version 7.7, Schrodinger, LLC) using hybrid density functional theory with Becke's three-parameter exchange potential and the Lee–Yang–Parr correlation functional (B3LYP) [41, 42] using basis set 3-21G* level [43-46].

Molecular docking

After ensuring that protein and ligands are in correct form, molecular docking of the optimized ligands onto the γ-tubulin dimer was performed using Glide (version 4.5, Schrodinger, LLC). The receptor-grid file was generated using grid receptor generation program with van der Waals scaling of 0.4 Å. A grid box size of 10 Å each for the bounding and enclosing boxes were generated at the centroid of the predicted binding sites (using SiteMap, version 2.4, Schrodinger, LLC) [47]. The ligands were first docked using the "standard precision" method and further refined using "extra precision" Glide algorithm [47-49] (Table 4). Single best conformation for each ligand–protein complex was selected for further molecular modeling calculations.

Table 4: Molecular docking evaluation of binding sites. All the three ligands were docked onto the 10 predicted binding sites of γ-tubulin dimer complex. The binding sites that showed better docking score with all the ligands were selected as the probable sites of interaction of these ligands on γ-tubulin dimer complex. On the basis of docking score, site 6 was selected.

Ligand	Site1	Site2	Site3	Site4	Site5	Site6	Site7	Site8	Site9	Site10
Amino	-2.81	-2.9	-3.48	-3.36	-3.1	**-3.55**	-1.88	-2.54	-3.08	-3.61
Bromo	-2.54	-2.94	-3.09	-2.7	-2.42	**-4.23**	-1.66	-2.48	-2.36	-3.82
Noscapine	-1.63	-4.26	-3.91	-3.97	-1.84	**-2.67**	-2.74	-2.14	-1.93	-3.88

Molecular dynamics simulations and binding affinity calculations.

The protein ligand complexes obtained after molecular docking were then simulated for 10 ns in Amber11 using the parameters as described in chapter 1. Before simulation the missing parameters for all four ligands were estimated with the antechamber programs [50] implemented in Amber 11. AM1-BCC charge model was used to calculate the atomic point charges [51]. Missing hydrogens were added and FF99SB forcefield was employed to assigned parameters to the complex of γ-tubulin dimer, while GAFF forcefield was used to assigned the parameters to each ligand using tleap module available in Amber 11. Binding affinity of noscapinoids at the γ-γ tubulin binding interface was then calculated using MM-PBSA and MM-GBSA methods.

Per residue energy decomposition

The contribution of each amino acid residue of the γ-tubulin dimer was calculated to identify those residues which show strong interaction with noscapinoids. These calculations were performed using MM-GBSA method implemented in Amber 11.

Results and discussions

Theoretical binding affinity calculations

The binding affinity of all three noscapinoids was calculated using MM-PBSA and MM-GBSA methods as described in chapter 1. All three noscapinoids displayed stable interaction throughout simulations (Figure 12 and 13). Bromo-noscapine showed the best binding affinity followed by noscapine and amino noscapine (Table 5). This could be attributed to the formation of hydrogen bonds between bromo-noscapine and surrounding amino acid residues(Figure 14).

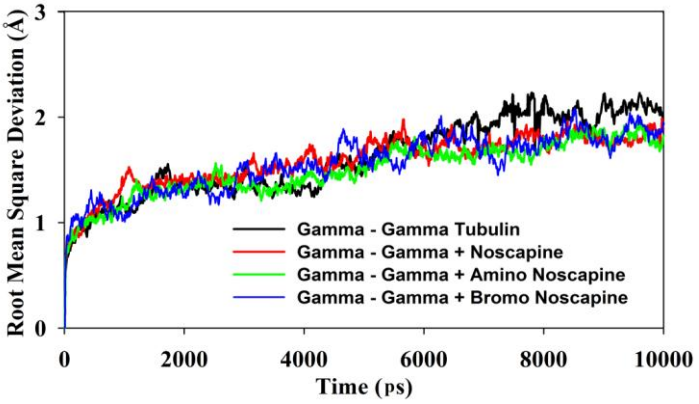

Figure 12: Root mean square daviation. The root mean square deviations (RMSD) of Cα atoms of the γ-tubulin dimer in the free form and bound form with different ligands (noscapine, amino-noscapine and bromo-noscapine) during the entire duration of MD simulation.

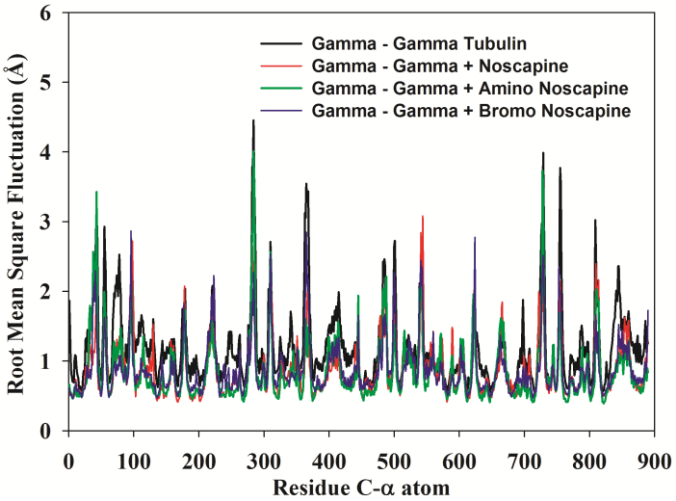

Figure 13: Root mean square fluctuation (RMSF) of Cα atoms. RMSF of residues in γ-tubulin dimer in the free form and in the bound form with different ligands (noscapine, amino-noscapine, bromo-noscapine) during the entire duration of MD simulation. The residues with higher RMSF tend to show more flexibility. The residues in the bound form show a small degree of flexibility when compared with free γ-tubulin dimer.

Table 5: Calculated binding free energy between GCP4 and γ-tubulin. Binding free energy calculated using MM-GBSA and MM-PBSA to ascertain the strength of interaction between GCP4 and γ-tubulin for both dimer 1 and dimer 2. The major energy components like van der Waals, electrostatic, polar solvation and non-polar solvation, contributing to the binding free energy were also estimated.

Contribution	Nos (kcal/mol)	A-Nos (kcal/mol)	Br-Nos (kcal/mol)
ΔE_{INT}	0.00	0.00	0.00
ΔE_{VDW}	-47.74	-54.15	-55.17
ΔE_{ELE}	-121.68	-108.00	-139.56
$\Delta E_{GAS/\Delta E\ MM}$	-169.41	-162.14	-194.72
ΔG_{PB}	142.84	141.70	160.60
ΔG_{SOL-NP}	-3.28	-3.55	-3.48
$\Delta G_{SOLV.PB}$	139.56	138.15	157.12
$\Delta G_{ELE.PB}$	17.89	30.15	17.56
$H_{TOT.PB}$	**-29.85**	**-23.99**	**-37.60**
G_{GB}	139.59	129.89	156.21
$G_{SOLV.GB}$	134.84	124.58	151.08
$G_{ELE.GB}$	17.91	21.89	16.65
$H_{TOT.GB}$	**-34.57**	**-37.56**	**-43.64**

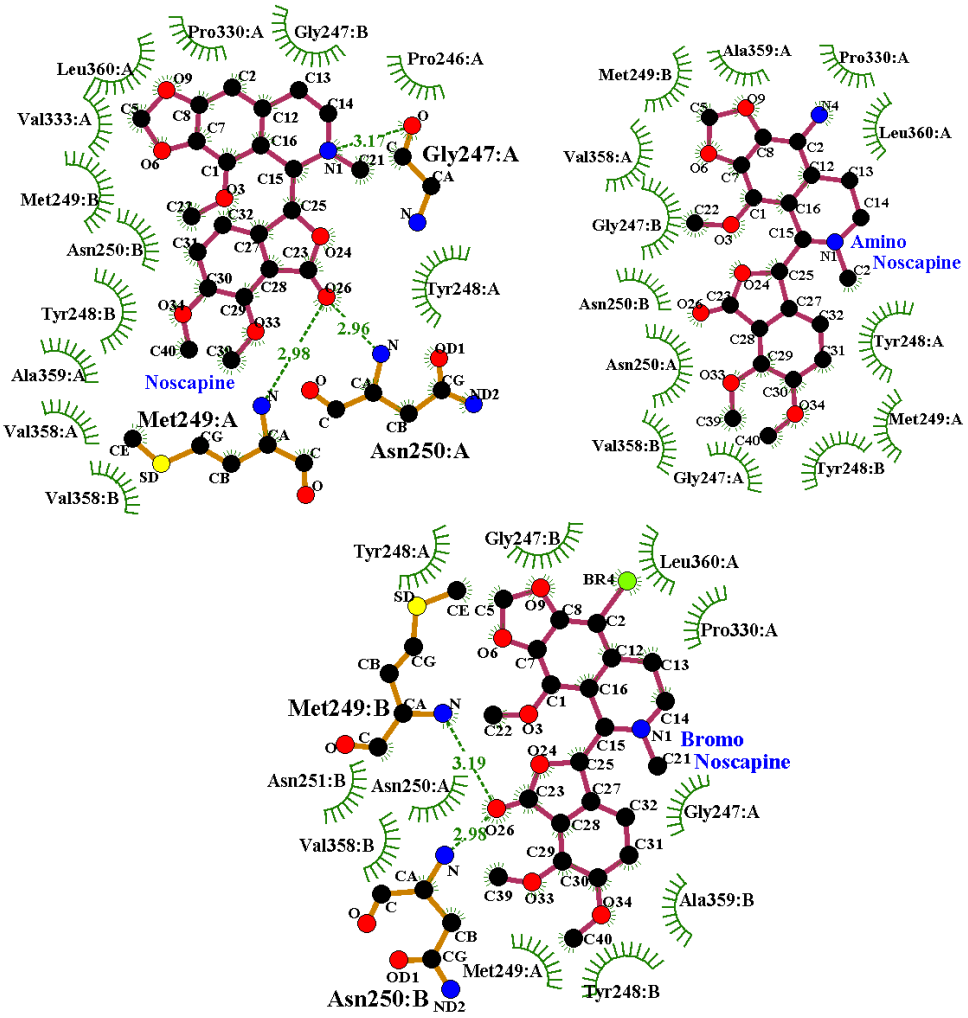

Figure 14: Binding modes of noscapinoids. Noscapinoids (Noscapine, Amino-Noscapine and Bromo-Noscapine) docked into γ-tubulin dimer.

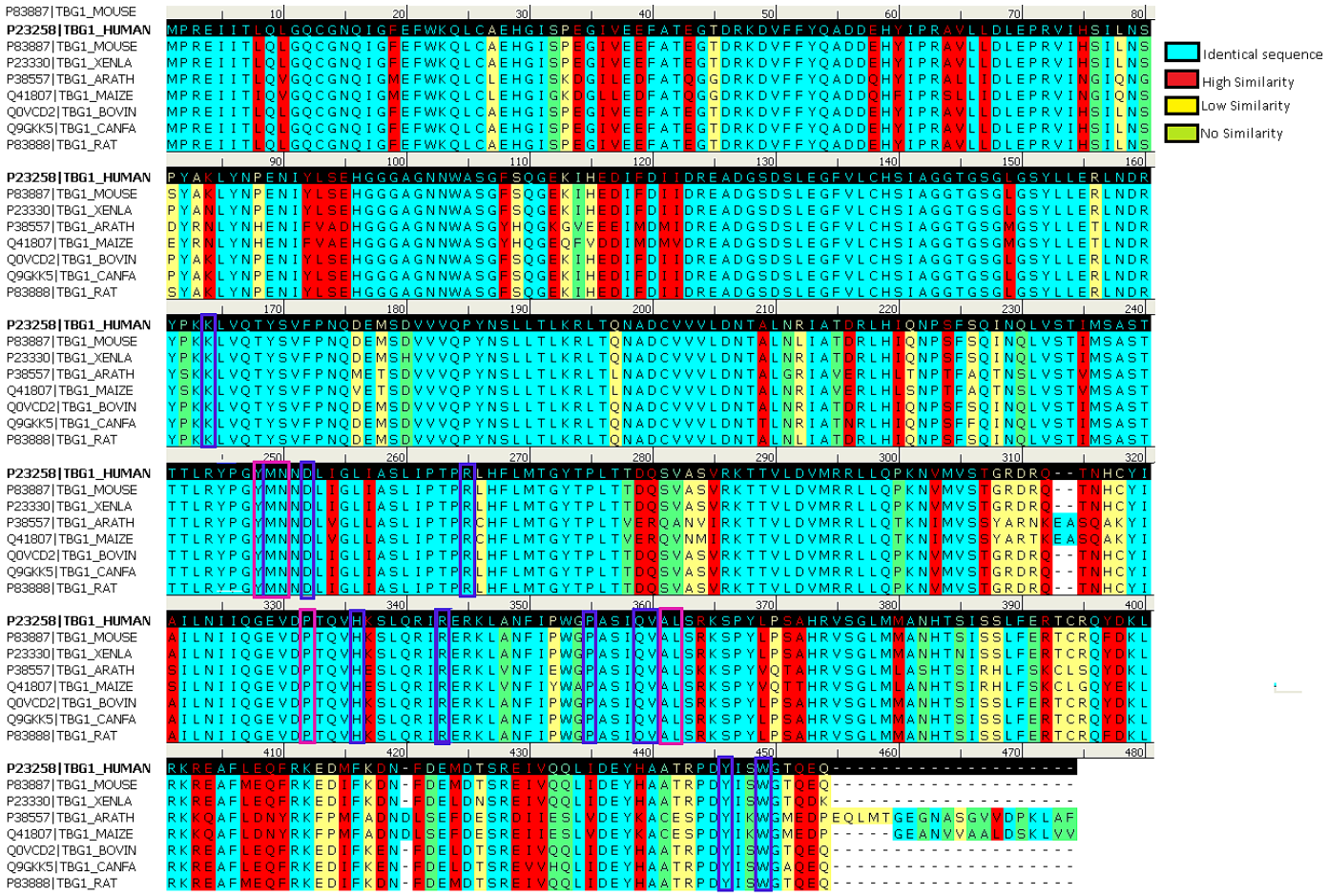

Figure 15: Multiple sequence alignment of γ-tubulin. γ-tubulin sequence show high level of homology across different species. The residues in the cyan region are identical. The residues enclosed with blue rectangle were identified as hotspot amino acids at the γ-γ tubulin dimer while those enclosed in magenta rectangle were observed to make strong contribution while binding with noscapinoids.

Conclusion

In this study, the binding modes of the three noscapinoids with the γ-tubulin dimer were illustrated using MD simulation and binding free energy calculations. All three ligands lodged themselves in the pockets located very close to the binding interface of the γ-tubulin dimer. All three ligands showed stable interaction throughout the simulations however the best binding affinity was calculated for bromo-noscapine. The binding modes of noscapine and bromo-noscapine are quite similar with both the drugs showing strong interaction with Tyr248, Met249, Asn250 of γ-tubulin. Multiple sequence alignment analysis showed the amino acid residues which interact with noscapinoids were observed to lie in the highly conserved regions. Therefore, if these drugs can interfere with a subset of the hotspot amino acids they might be able to perturb some of the interactions between γ-tubulin units in the γTuRC and further destabilize the γTuRC. Nevertheless, our results offer noscapinoids an important possible chemical framework for the further design of more potent compounds.

CHAPTER 3 – Molecular basis of interaction of γ-tubulin and GCP4

The initiation of microtubule assembly within cells is guided by a cone shaped multi-protein complex containing γ-tubulin and at least five other γ-tubulin-complex proteins (GCPs) i.e., GCP2, GCP3, GCP4, GCP5, and GCP6. The rim of complex is a ring of γ-tubulin molecules that interacts, via one of its longitudinal interfaces, with GCP2, GCP3 or GCP4 of γ-tubulin ring complex (γTuRC) and, via other interface, with α/β tubulin dimers recruited for the microtubule lattice formation. These interactions however, are not well understood. Therefore, in this study we used molecular modelling and MD simulations, combined with MM-PBSA and MM-GBSA computational methods to understand atomic interactions between γ-tubulin and GCP4. We simulated two conformations of γ-tubulin-GCP4 complex for 10 ns and calculated the binding free energy. These values points to very robust interactions between GCP4 and γ-tubulin. We also identified amino acids crucial for the interaction of γ-tubulin with GCP4, called hotspots, by computational alanine-scanning mutagenesis.

Material & Methods

Molecular System

A pseudo atomic model of the GCP4 and γ-tubulin tetramer was obtained from Georges Czaplicki, from the Universite´ de Toulouse, UPS, Toulouse, France. The coordinates of the atoms were obtained by fitting the crystal structures of GCP4 and γ-tubulin (PDB_ID 3RIP and 3CB2 respectively) onto the 8 Å cryo-electron microscopy (EM) reconstruction of the *Saccharomyces cerevisiae* γ–tubulin small complex (γ-TuSC). The GCP4 and γ-tubulin tetramer structure was then prepared using protein preparation wizard (PPrep) workflow in Schrodinger package.

Molecular Dynamics Simulation

Since we intended to understand the molecular interaction between GCP4 and γ-tubulin, we split the tetramer into two dimers (dimer 1 and dimer 2), each having a unit of GCP4 and γ-tubulin. Both dimers were then MD simulated using Amber 11.0 and Ambertools 1.5 keeping the procedue and parameters consitent with those described in chapter1.

Calculation of binding free energy between GCP4 and γ-tubulin

Binding free energy calculations were carried out using the conventional MM-PBSA and MM-GBSA approaches using Amber 11. A total of 500 snapshots were extracted, every 10 ps from the last 5 ns of the MD trajectory. For each snapshot, the free energy was calculated for each molecular species (complex, protein and ligand). Conceptually the binding free energy can be calculated as :

$$\Delta G_{bind} = \Delta G_{complex} - [\Delta G_{Rec} + \Delta G_{lig}]$$

Per residue energy contribution

In order to identify those residues wich play a more substantial role in the binding of GCP4 with γ-tubulin, energy contribution of each amino acid in the complex was determined. Energy decompostion method, implemented in Amber 11, was employed on the 500 frames extracted every 10 ps from last 5 ns of simulation using the MM-GBSA method. The residues contributing more than 3 kcal/mol were considered very significant for the binding of GCP4 with γ-tubulin and these residues were designated as hotspot amino acids.

Alanine scanning mutagenesis

The hotspot residues identified in both the dimer (18 in each dimer) were mutated to Alanine, one by one to recalculated the binding free energy using the MM-GBSA and MM-PBSA methods. A total of 18 alanine scanning runs were carried out for each dimer to calculate $\Delta\Delta G_{bind}$ given by:

$$\Delta\Delta G_{bind} = \Delta_{Gmutant} - \Delta G_{wild\ type.}$$

Results and discussions

The dimers of GCP4 and γ-tubulin were simulated for 10 ns and the resultant trajectories were utilized for the calculation of binding free energies using the MM-GBSA and MM-PBSA methods. The binding free energies and their components between GCP4 and γ-tubulin were calculated independently for both dimer 1 and dimer 2 and presented in Table 6. Hotspot amino acids were identified using the MM-GBSA analysis (Figure 16 and 17). The contributions of individual amino acids were also calculated (Table 7 and Figure 18).

Table 6: Calculated binding free energy between GCP4 and γ-tubulin. Binding free energy calculated using MM-GBSA and MM-PBSA to ascertain the strength of interaction between GCP4 and γ-tubulin for both dimer 1 and dimer 2. The major energy components like van der Waals, electrostatic, polar solvation and non-polar solvation, contributing to the binding free energy were also estimated.

Contribution	Dimer1	Dimer 2
ΔE_{INT}	0.00	0.00
ΔE_{VDW}	-274.8	-193.9
ΔE_{ELE}	54.52	106.9
ΔE_{GAS}	-220.3	-87.04
ΔG_{PB}	76.53	-17.17
ΔG_{SOL-NP}	-28.95	-20.40
$\Delta G_{SOLV,PB}$	47.57	-37.57
$\Delta G_{ELE,PB}$	131.1	89.69
$H_{TOT,PB}$	-172.7	-124.6
G_{GB}	67.49	17.78
$G_{SOLV,GB}$	31.77	-6.530
$G_{ELE\ GB}$	122.0	124.6
$H_{TOT,\ GB}$	-188.5	-93.58

Table 7: Energy decomposition. Decomposition of calculated $\Delta G_{bind,GB}$ (kcal/mol) on per residue basis into van der Waals, electrostatic, polar solvation and non-polar solvation energy components for the hotspot amino acids.

Chain	Residue	$\Delta E_{i,vdw}$	$\Delta E_{i,ele}$	$\Delta G_{i,sol\ GB}$	$\Delta G_{i,sol\text{-}np}$	$\Delta H_{i,tot,GB}$
Dimer1						
GCP4 (Chain A)	ASP359	-0.631	17.37	-23.70	-0.112	-7.067
	GLU367	-2.371	-0.364	-9.287	-0.867	-12.89
	LEU404	-4.668	1.608	-0.628	-0.807	-4.494
	TRP514	-4.242	-1.422	2.171	-0.512	-4.005
	ARG515	-3.683	-91.82	86.54	-1.052	-10.02
	TYR529	-5.310	-13.17	9.977	-0.674	-9.178
	GLN532	-7.644	-8.654	13.10	-0.918	-4.113
	VAL533	-7.307	-4.964	5.069	-1.066	-8.268
	GLU537	-2.808	-1.211	-4.155	-0.459	-8.634
γ-tubulin (Chain B)	ARG2	-0.109	-85.92	78.97	-0.015	-7.074
	ARG46	-1.858	-97.65	93.88	-0.333	-5.961
	PRO261	-3.317	-6.037	6.473	-0.463	-3.343
	GLU326	-2.955	39.44	-39.92	-0.669	-4.112
	ASP328	-5.678	54.37	-52.29	-0.648	-4.245
	PRO329	-4.535	-4.084	4.201	-0.693	-5.111
	VAL357	-2.325	-3.763	2.728	-0.220	-3.580
	ARG361	-0.912	-88.03	82.05	-0.586	-7.472
	TRP445	-5.106	-40.32	41.29	-1.429	-5.566
Dimer 2						
GCP4 (Chain A)	GLU367	-1.559	29.45	-32.59	-0.379	-5.077
	TRP514	-5.879	-5.064	5.921	-0.772	-5.794
	ARG515	-4.269	-89.53	91.01	-0.946	-3.733
	ASN518	-3.379	-8.308	8.679	-0.478	-3.486
	PHE522	-6.696	-2.215	4.432	-1.109	-5.587
	ASN526	-3.109	-9.237	8.191	-0.470	-4.626
	TYR529	-6.190	-6.725	7.210	-0.948	-6.653
	TYR530	-4.573	-4.544	5.883	-0.694	-3.928
	SER538	-1.546	-4.497	3.018	-0.341	-3.367
γ-tubulin (Chain B)	ARG46	-1.773	-73.68	71.89	-0.501	-4.065
	MET248	-4.035	-2.106	3.273	-0.451	-3.319
	ASN249	-6.549	-7.999	11.72	-1.091	-3.920
	ILE 253	-3.722	-1.292	2.096	-0.783	-3.701
	PRO263	-2.992	0.623	-0.331	-0.586	-3.286
	PRO329	-3.847	-3.891	4.235	-0.469	-3.972
	HIS333	-4.105	-13.94	13.03	-0.722	-5.734
	ARG361	-0.159	-78.57	72.75	-0.335	-6.312
	TYR442	-0.759	-10.51	8.001	-0.171	-3.442

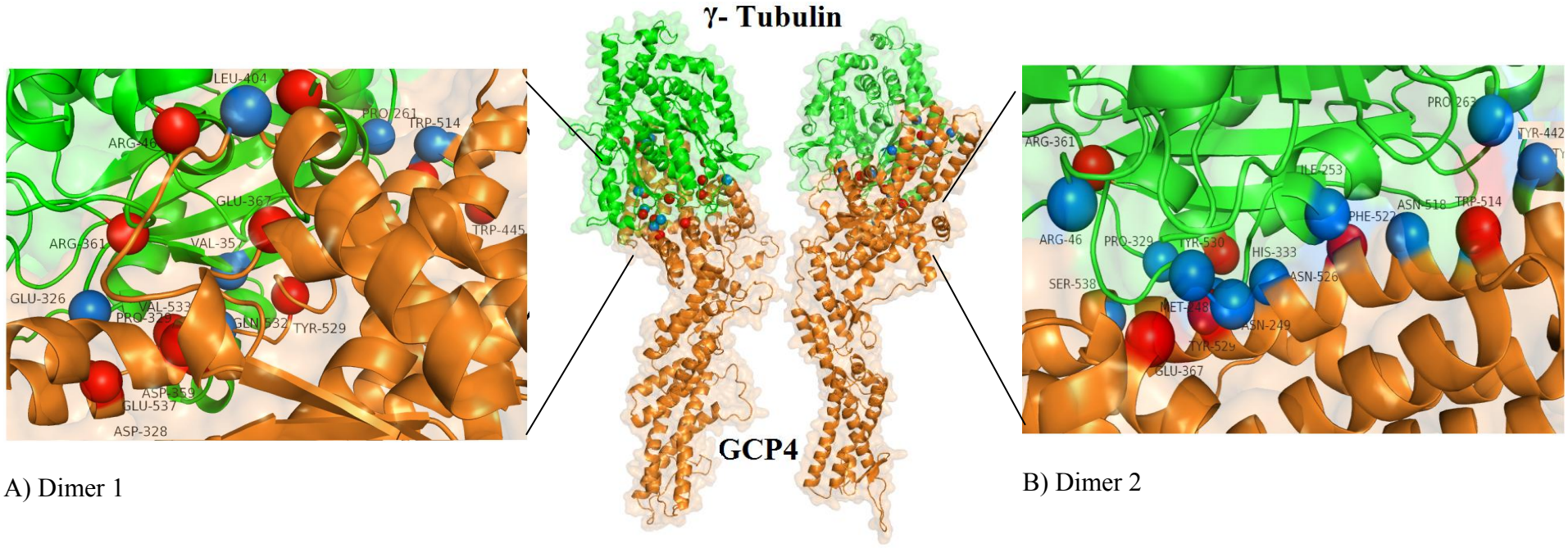

A) Dimer 1

B) Dimer 2

Figure 16: Spatial distribution of hotspot residues at the binding interface. Hotspot residues involve in the binding process of GCP4 and γ tubulin at the interface in the dimmer 1 (A) and dimer 2 (B) are represented in the three dimensional space model of the complex. The hotspot residues contributing free energy of >5 kcal/mol are marked red, while the residues contributing free energy in between 3 kcal/mol and 5 kcal/mol are marked blue. In total nine residues each on the surface of GCP4 and γ-tubulin involve in the binding process in both dimmer 1 and dimmer 2. However, the residues are albeit different between both the dimers. This is the reason that the predictive binding free energies between both the dimmers are different. The binding free energy between GCP4 and γ-tubulin calculated in dimer 1 is much higher (-188.51 kcal/mol and -172.71 kcal/mol) compared to dimer 2 (-93.58 kcal/mol and -172.71 kcal/mol) based on both MM-PBSA and MM-GBSA methods, respectively.

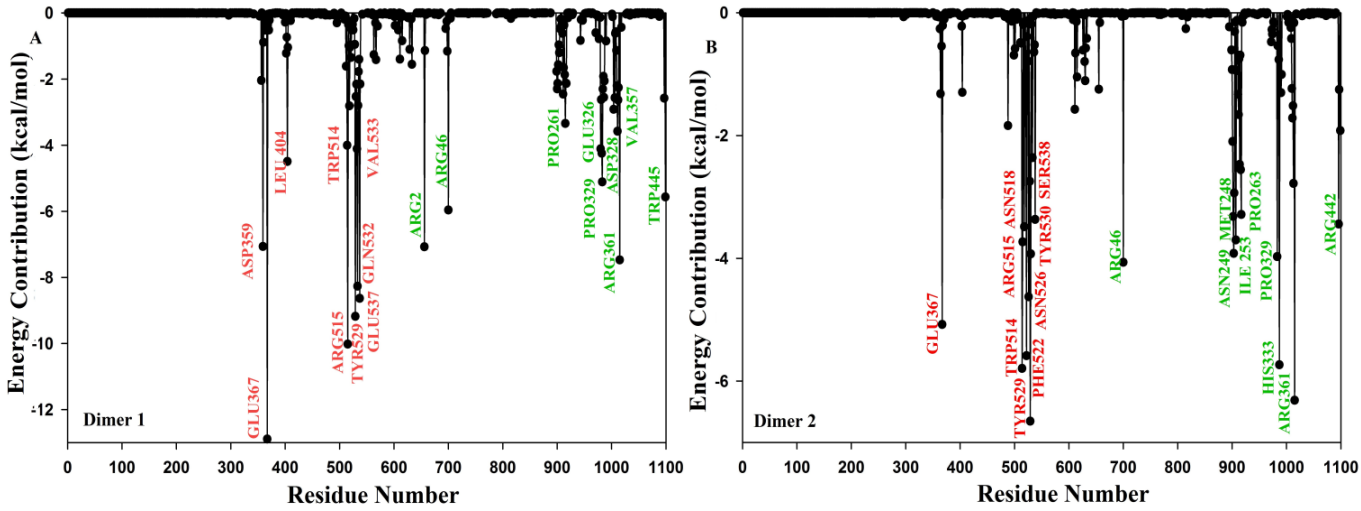

Figure 17: **Per residue free energy contribution of residues in the binding process of GCP4 and γ-tubulin.** Free energy contribution of each residue on the surface between GCP4 and γ-tubulin involve in the interaction in dimer 1 (A) and dimer 2 (B), calculated based on MM-GBSA. Only the residues contributing free energy of >3 kcal/mol (designated as hotspot amino acids) are labelled in the figure. The hotspot residues belonging to GCP4 are labelled red while those of γ-tubulin are labelled green.

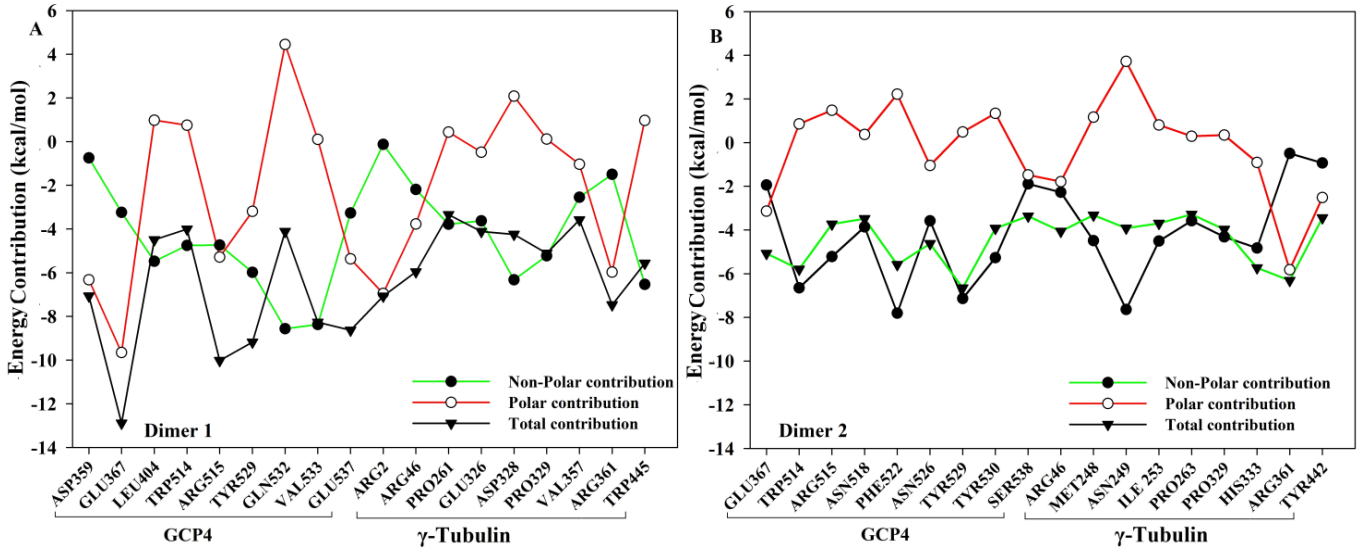

Figure 18: Polar and nonpolar energy contribution of hotspot residues. The decomposition of total energy contributions into polar and non-polar energy components of hotspot amino acids in the binding process of GCP4 and γ-tubulin in dimer 1 (A) and dimer 2 (B). For both GCP4 and γ-tubulin the hotspot amino acids make considerable nonpolar solvation contributions compared to the polar contributions. Polar interactions were calculated as sum of electrostatic (ΔEi,ele) and polar solvation (ΔGi,sol GB) energy components while the non-polar interactions were calculated as sum of van der waals (ΔEi,vdw) and non-polar solvation component (ΔGi,sol-np).

Table 8: $\Delta\Delta G_{bind}$ for hotspot amino acids. Computational alanine scanning mutagenesis was carried for all the 36 hotspot amino acids between GCP4 and γ-tubulin for both dimer 1 and dimer 2. Those amino acid residues which contributed more than 3 kcal/mol to the binding affinity of GCP4 and γ-tubulin complex were mutated to alanine, one by one, to determine $\Delta\Delta G_{bind}$. $\Delta\Delta G_{bind}$ was calculated as $\Delta_{Gmutant} - \Delta G_{wild\ type}$.

Chain	Residue	$\Delta\Delta G_{bind}$ (MM-GBSA)	$\Delta\Delta G_{bind}$ (MM-PBSA)
Dimer1			
GCP4 (Chain A)	ASP359	13.66	27.89
	GLU367	34.22	43.37
	LEU404	4.20	2.20
	TRP514	5.28	4.32
	ARG515	15.02	13.94
	TYR529	7.28	3.89
	GLN532	5.04	7.83
	VAL533	3.60	5.06
	GLU537	20.73	22.17
γ-tubulin (Chain B)	ARG2	17.52	32.50
	ARG46	16.33	26.46
	PRO261	1.14	1.09
	GLU326	3.07	4.29
	ASP328	19.11	21.64
	PRO329	3.00	0.92
	VAL357	0.04	0.65
	ARG361	15.41	14.71
	TRP445	2.42	1.54
Dimer 2			
GCP4 (Chain A)	GLU367	16.49	25.21
	TRP514	10.42	9.74
	ARG515	8.11	10.04
	ASN518	4.99	4.75
	PHE522	8.17	4.41
	ASN526	6.13	6.46
	TYR529	12.13	7.89
	TYR530	9.73	2.73
	SER538	4.16	5.43
γ-tubulin (Chain B)	ARG46	9.80	12.66
	MET248	5.28	6.19
	ASN249	4.73	8.95
	ILE 253	2.22	0.40
	PRO263	2.52	2.98
	PRO329	3.14	5.09
	HIS333	10.60	8.30
	ARG361	8.54	9.65
	TYR442	3.40	1.43

Conclusion

The current computational study provides insights into the interactions between GCP4 and γ-tubulin in two different conformations using molecular dynamics to calculate the binding free energy of binding in solvation and identifying key residues participating in the interactions. Computational alanine scanning mutagenesis analysis further verified hotspot amino acids. Mutation of every hotspot residue resulted in drop in binding affinity by a minimum of 0.4 kcal/mol (Table 8).

CHAPTER 4 – Noscapinoids binds at the interface between γ-tubulin and GCP4 complex pertaining to inhibition of microtubule formation.

In the endeavour to identify chemical leads that might interact at the interface between γ-tubulin and GCP4 and disrupt formation of microtubules; we found that noscapine and its derivatives fits well in a cavity close to the interface region. All noscapinoids displayed stable interaction throughout simulation. This offers a novel chemical scaffold for drugs near γ-tubulin-GCP4 interface pertaining to inhibition of microtubule initiation.

Ligand preparation

The molecular structure of the lead molecule, noscapine and two of its derivatives such as amino-noscapine and bromo-noscapine **1-3** (Figure 19) were built using molecular builder of Maestro (version 8.5, Schrodinger LLC). We also selected and built two compounds, NM87 and NM372 **4,5** (Figiure 19) as reference compounds, which have previously reported to bind specifically to the GCP4 and γ-tubulin interface. All these five structures **1-5** were energy minimized *in-vacuo* using Impact (version 5.6, Schrodinger, LLC).

Molecular docking

After ensuring that protein and ligands are in correct form, molecular docking of the optimized ligands onto the complex of GCP4 and γ-tubulin was performed using Glide (version 4.5, Schrodinger, LLC). The ligands were first docked using the "standard precision" method and further refined using "extra precision" Glide algorithm. A total of thirty structures with lowest energy conformations were then screened for favourable Glide docking score. Single best conformation for each ligand–protein complex was selected for further molecular modeling calculations (Table 9).

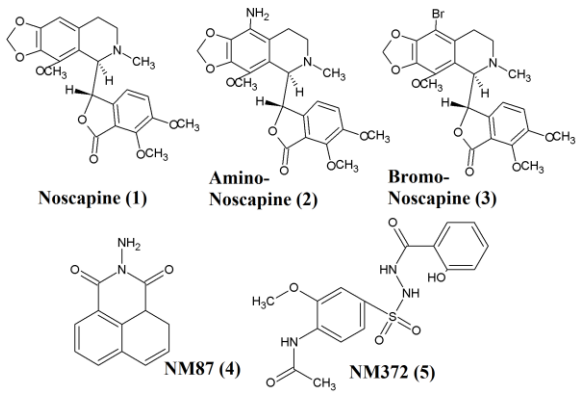

Figure 19: Molecular structure of the Noscapinoids: Noscapine (1), Amino-noscapine (2), Bromo-noscapine (3) and two reference compounds NM87 (4) and NM372 (5) used in the study. Both the reference compounds are previously reported to bind specifically onto the GCP4 and γ-tubulin interface.

Structure preparation of docked complexes

The complexes obtained after molecular docking required some structure preparation to make them suitable for molecular dynamics simulations in Amber 11. This was done using the methods and parameters as described for docked complexes in chapter 2.

Molecular dynamics simulation of docked complexes

The parameter for the compounds **1-5** were estimated using antechamber program in Amber 11 simulation package. All the docked complexes were subjected to three rounds of minimization followed by heating, density equilibration and pressure equilibration. The equilibrated structure was then MD simulated for 10 ns. Similar methods, parameters and the constraints were used as described above for the MD simulation of GCP4 and γ-tubulin complex. The structures were recoreded every 1 ps resulting in a trajectory with 10,000 frames.

Calculation of binding free energy of docked complexes

The calculation of binding free energy between the ligand and the complex of GCP4 and γ-tubulin was carried out using the MM-GBSA and MM-PBSA method. Similar scoring sheme was used for the calculation of binding free energy as described above between GCP4 and γ-tubulin. Free energy of binding was calculated as the ensemble average of the binding free energy of a total of 500 snapshots, extracted every 10 ps from the last 5 ns of the MD simulation trajectory.

Decomposition of ligand-residue interaction of docked complexes

The energy contribution of each residue in docked complexes was estimated using the MM-GBSA decomposition process in Amber 11.0 over the 500 frames obtained every 10 ps from the last 5 ns of simulation. The binding energy of each ligand-residue pair includes three energy terms: the van der Waals contribution (ΔE_{vdw}), the electrostatic contribution (ΔE_{ele}) and the solvation contribution (ΔE_{sol}). All the energy components are calculated using the same frames obtained from MD trajectories that were used for calculation of binding affinity.

Results and discussion

Molecular dynamics trajectory of 10,000 frames was generated (1 frame every 1 ps) during 10 ns simulation for all docked complexes. The relative fluctuation in the RMSD of the Cα atoms is very small after 400 ps, revealed that each system reaches equilibrium at 400 ps (Figure 20). The root mean fluctuation analysis revealed that the residues in the bound form show a small degree of flexibility when compared with free GCP4 and γ-tubulin complex (Figure 21).

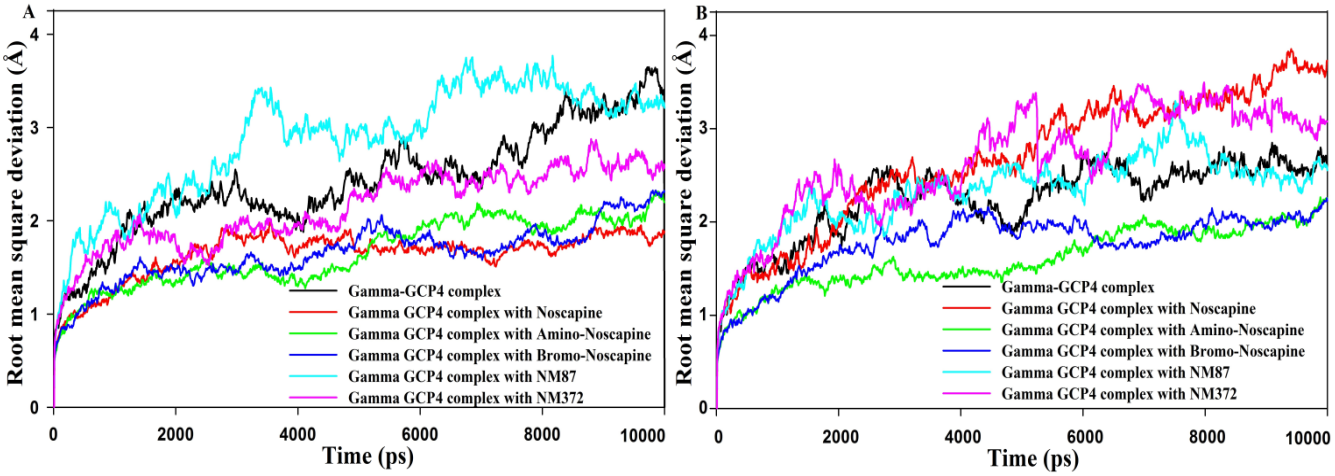

Figure 20: Root mean square deviation. The root mean square deviations (RMSD) of Cα atoms in the GCP4 and γ-tubulin complex in dimer 1 (A) and dimer 2 (B) in the free form and bound form with different ligands (noscapine, amino-noscapine, bromo-noscapine, NM87 and NM372) during the entire duration of MD simulation.

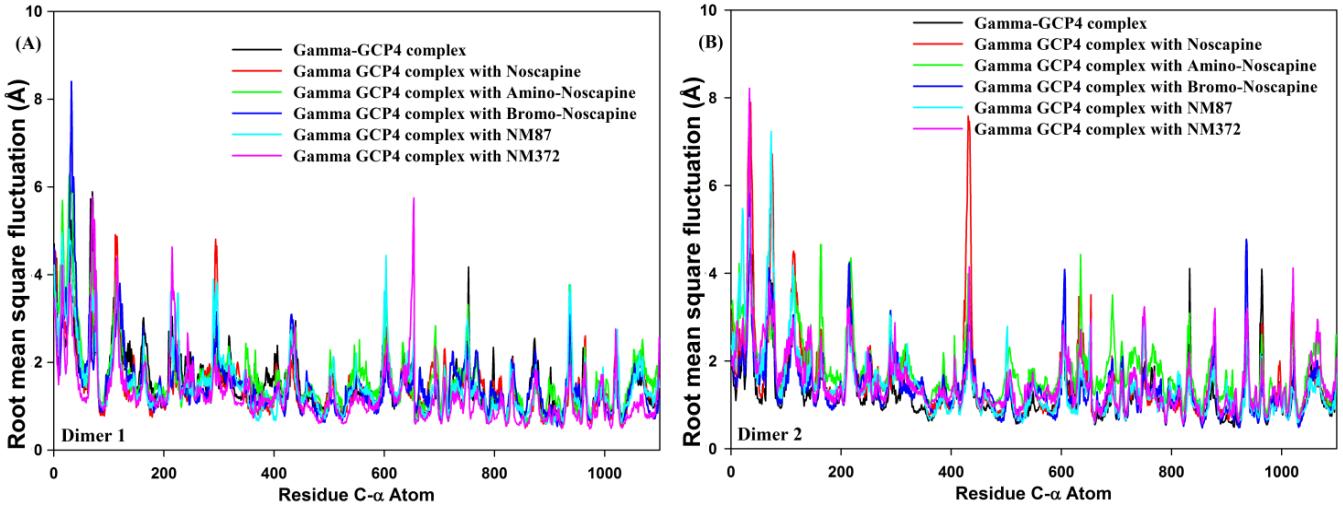

Figure 21: Root mean square fluctuation (RMSF) of Cα atoms. RMSF of residues in the complex of GCP4 and γ-tubulin in dimmer 1 (A) and dimmer 2 (B) in the free form and in the bound form with different ligands (noscapine, amino-noscapine, bromo-noscapine, NM87 and NM372) during the entire duration of MD simulation.

Per residue energy decomposition

Energy contribution of each residue in the interface between GCP4 and γ-tubulin among both dimer 1 and dimer 2 was calculated using the MM-GBSA method to investigate the details of protein-protein interactions at the atomic level (Figure 22). We identified 18 hotspot amino acids that have the highest impact (per residue contribution > 3 kcal/mol) on the GCP4 and γ-tubulin interaction (Figure 22). The spatial distributions of these hotspots at the binding interface between GCP4 and γ-tubulin are shown in Figure 23 for both the dimers.

Table 9: Glide docking scores. After predicting the binding sites, extra-precision docking was performed using Glide XP dock protocol implemented in Schrodinger package. XP_{score} (kcal/mol) of noscapenoids (noscapine, amino-noscapine, bromo-noscapine, NM87 and NM372) with GCP4 and γ-tubulin hetero-dimer are presented in the table. Noscapinoids showed better docking score compared to the reference molecules, NM87 and NM372.

(A). Site 1					
Ligand	**Glide e_{vdw}**	**Glide e_{coul}**	**Glide Emodel**	**Glide energy**	**XP Score**
Noscapine	-22.72	-4.34	-31.95	-27.06	-7.59
Amino	-9.18	-4.95	40.25	-14.13	-8.56
Bromo	-26.88	-5.67	-44.30	-32.55	-9.08
NM87*	-23.46	-2.68	-31.04	-26.13	-6.74
NM372*	-37.18	-10.93	-69.51	-48.11	-7.28
(B). Site 2					
Ligand	**Glide e_{vdw}**	**Glide e_{coul}**	**Glide**	**Glide energy**	**XP**
Noscapine	-38.25	-8.17	-53.86	-46.41	-6.83
Amino	-27.64	-11.70	-51.58	-39.34	-8.73
Bromo	-38.84	-10.11	-47.14	-48.95	-9.19
NM87*	-24.69	-4.28	-36.71	-28.97	-6.66
NM372*	-36.61	-7.20	-63.52	-43.82	-7.70

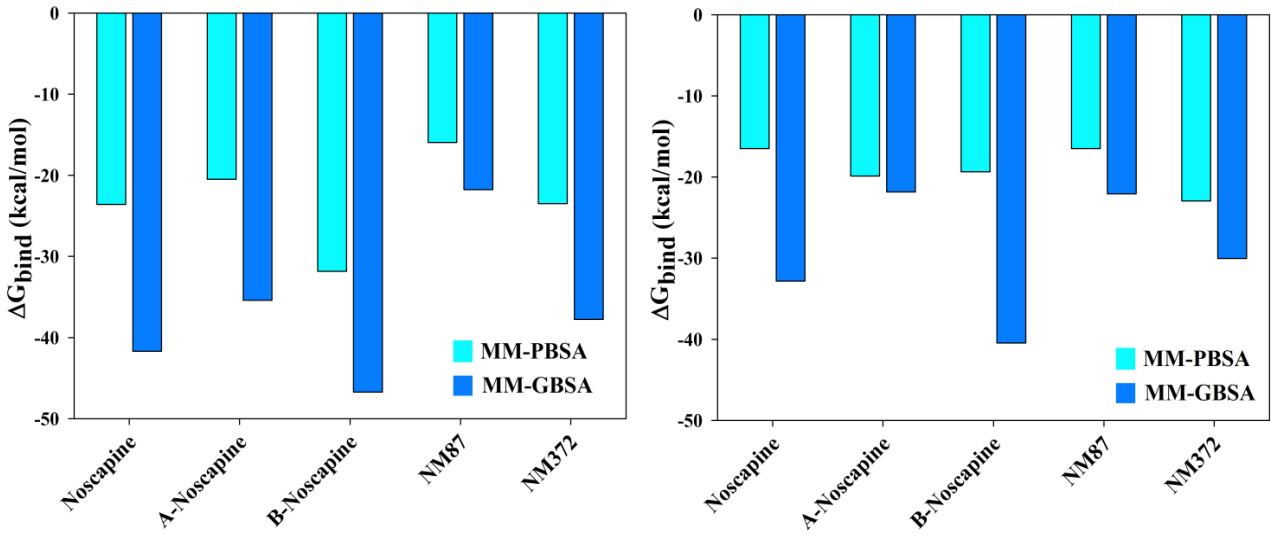

Figure 22: 2-D ligplot: A 2-D representation of the binding mode of drugs drugs (a: Noscapine, b: Amino-Noscapine and c: Bromo-Noscapine) with the complex of GCP4 and γ-Tubulin. In the images 'A' denotes the residues of GCP4 and 'B' denotes the residues of γ-Tubulin.

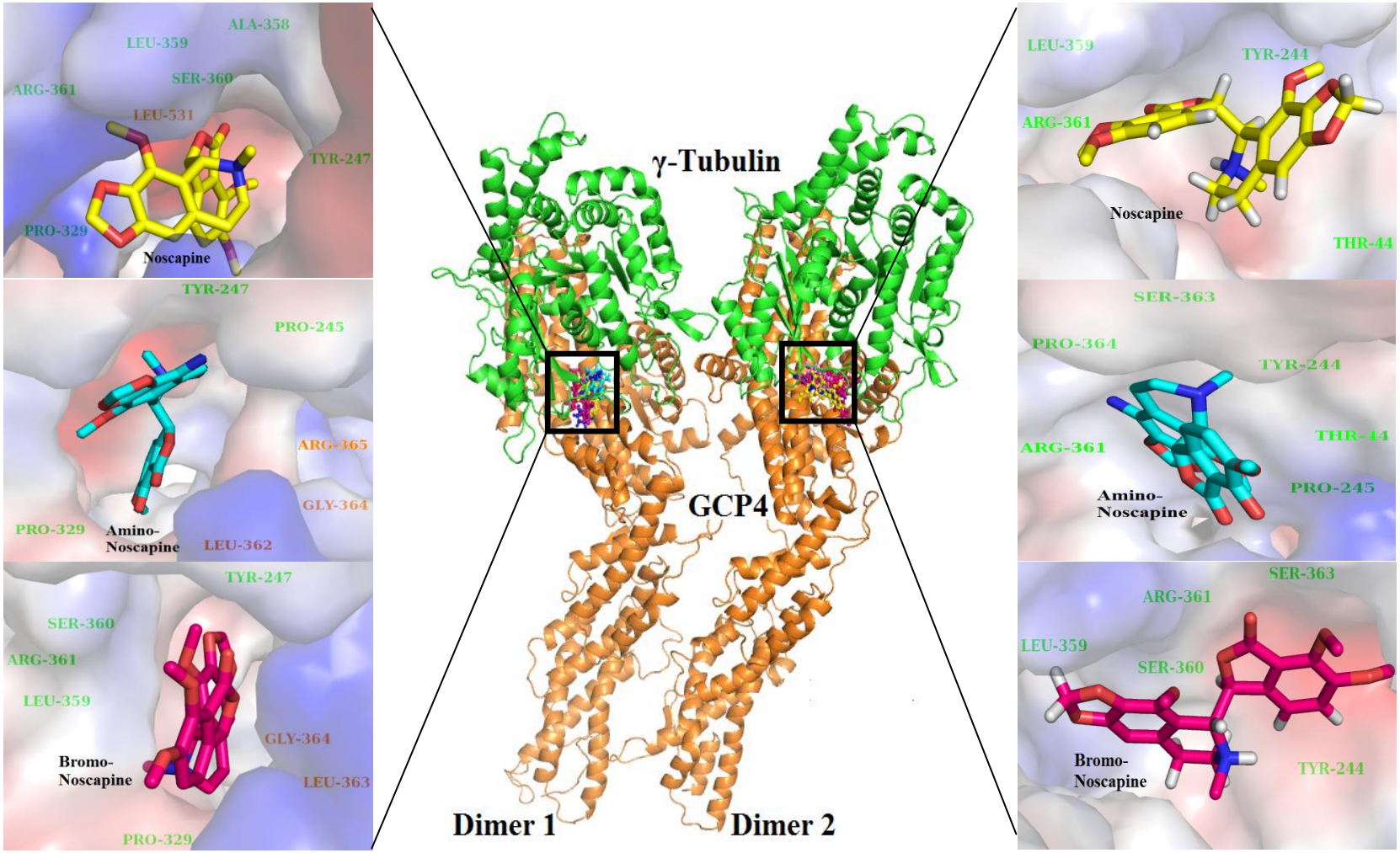

Figure 23 a: Binding modes of noscapinoids. Noscapinoids (Noscapine, Amino-Noscapine and Bromo-Noscapine) docked into dimer 1 and dimer 2. The zoomed views show the binding modes of the noscapinoids along. The residues which show contribution of more than -1 kcal/mol to the binding affinity are labeled green for γ-tubulin and orange for GCP4.

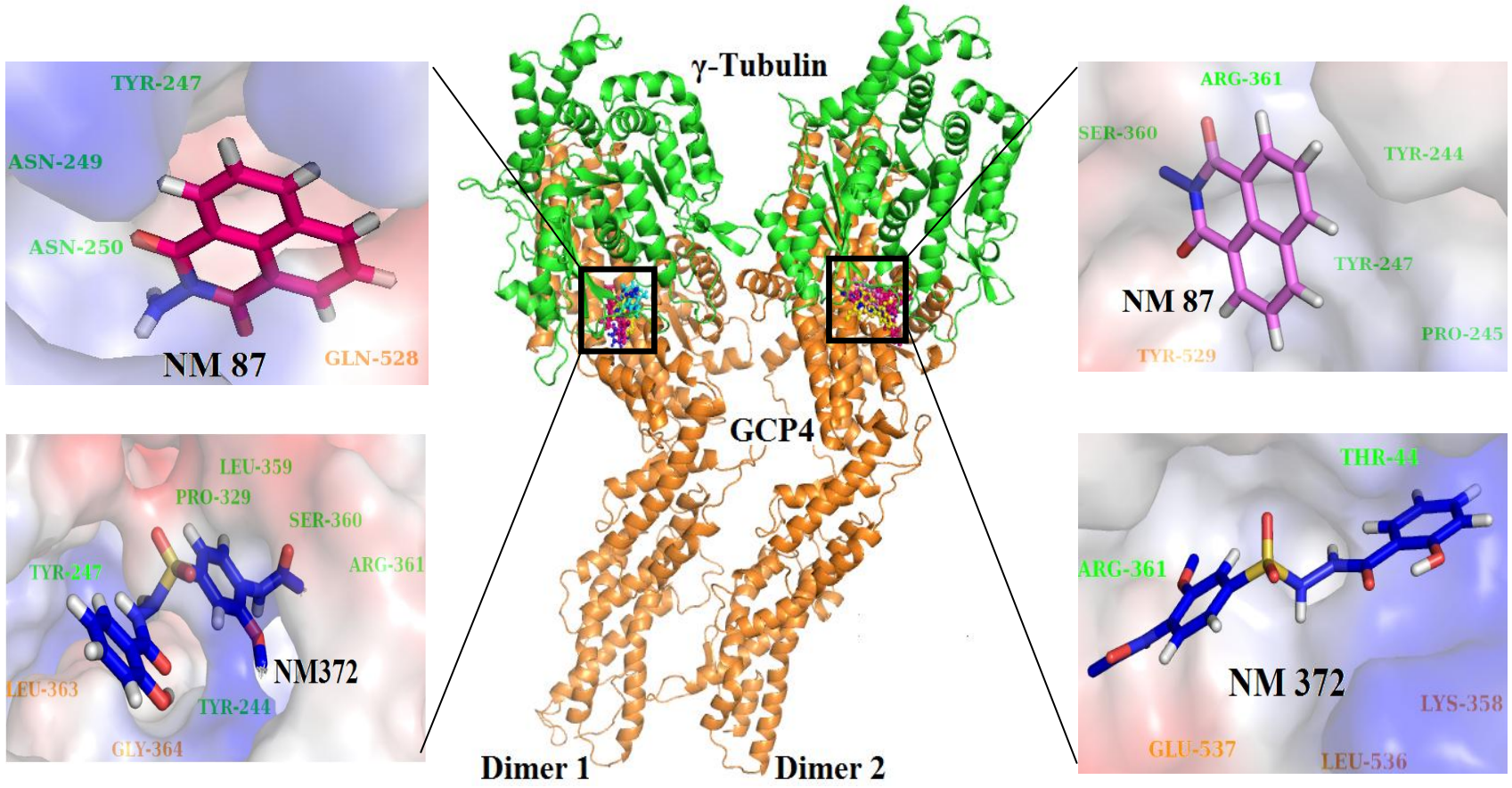

Figure 23 b: Binding modes of Reference molecules. Noscapinoids (Noscapine, Amino-Noscapine and Bromo-Noscapine) and reference molecules (NM 87 and NM 372) docked into dimer 1 and dimer 2. The zoomed views show the binding modes of the reference molecules. The residues which show contribution of more than -1 kcal/mol to the binding affinity are labeled green for γ-tubulin and orange for GCP4.

Conclusion

The complexes GCP4 and γ-tubulin were subjected to molecular docking with potential anti-cancer drug, noscapinoid and two of its derivatives amino-noscapine and bromo-noscapine. The binding modes of the three noscapinoids with the GCP4 and γ-tubulin dimers were further illustrated using MD simulation and binding free energy calculations. All three drugs lodged themselves in the pockets located very close to the binding interface of the GCP4 and γ-tubulin. The molecular interaction of all the three drugs are leveraged more towards γ-tubulin. The binding modes of noscapine and bromo-noscapine are quite similar with both the drugs showing strong interaction with Tyr247, Pro329, Leu359, Ser360 and Arg361 of γ-tubulin in dimer 1. Both drugs also displayed similar interactions with Tyr244, Leu359 and Arg361 in dimer 2. Pro329 and Arg361 are also two important identified hotspot amino acids in the interaction of GCP4 and γ-tubulin. We also observe that in almost all complexes the drug makes H-bond with Arg361. Therefore, if these drugs can interfere with a subset of the hotspot amino acids they might be able to perturb some of the interactions between GCP4 and γ-tubulin and further destabilize the γTuRC. Nevertheless, our results offer noscapinoids an important possible chemical framework for the further design of more potent compounds.

CHAPTER 5 – Molecular interactions of γ-tubulin with α/β microtubules.

γ-tubulin is indispensible for the microtubule spindle function in mitosis and its absence causes cell death. According to the template model γ-tubulin directly interacts, via one of its longitudinal interfaces, with the GCP2, GCP3 or GCP4 and, via its other interface, with the α/β tubulin dimers (Figure 1). In this study we elucidate the mode and mechanism of interaction of γ-tubulin with α/β tubulin.

Materials and Methods

Molecular system

A pseudo atomic model of the α/β tubulin tetramer was obtained from David B. Wells, University of Illinois, Urbana, Illinois; while the coordinates of GCP4 and γ-tubulin tetramer was obtained from Georges Czaplicki, from the Universite´ de Toulouse, UPS, Toulouse, France (Figure 24). As γ-tubulin interacts with α/β tubulin at the minus end, we deleted one of the β-tubulin to obtain the seam conformation. Since no crystal structure of the complete complex (comprising of α/β tubulin, γ-tubulin and GCPs) is available, we followed a two step process that involved initial protein-protein docking using Zdock (version 2.3) followed by refinement of docked complex using Rdock (25). Zdock is a rigid-body docking algorithm based on the principle of pair wise shape complementarity (PSC), electrostatic and desolvation parameters. In step 2, the top scoring poses obtained from Zdock were energy minimized using CHARMM force field. The binding affinity ($\Delta G_{binding}$) between the protein complexes was predicted using Rdock scoring function which is the sum of desolvation and electrostatics contribution.

$$\Delta G_{binding} = \Delta G_{ACE} + \beta \text{ X } \Delta G_{elec}$$

where β is a scaling factor, a value of 0.9 was used in this study. The conformation with least RDock score was then selected for further molecular dynamics studies.

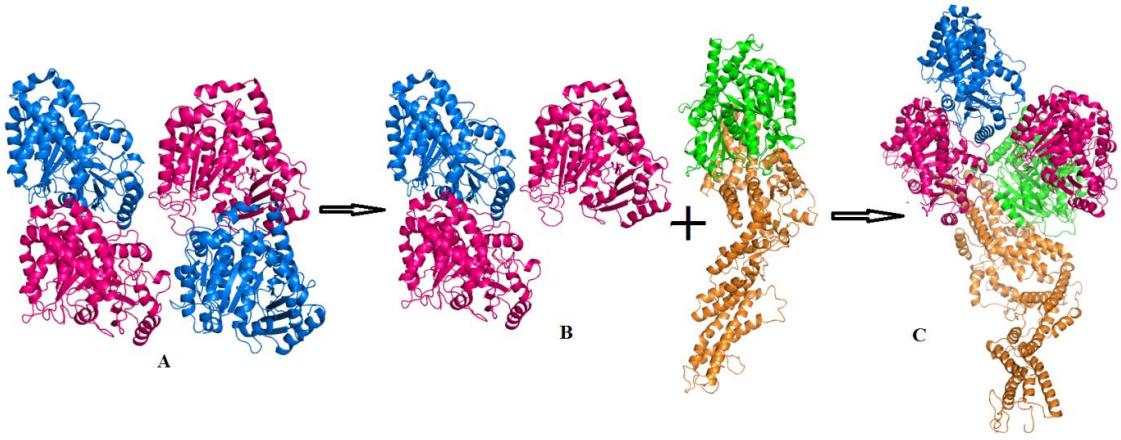

Figure 24: Preparation of molecular system. A: The coordinates of ‘α/β tubulin tetramer obtained from David B. Wells *et.al*. from University of Illinois. B: Protein complexes for docking. C: The resulting docked complex obtained after Rdock.

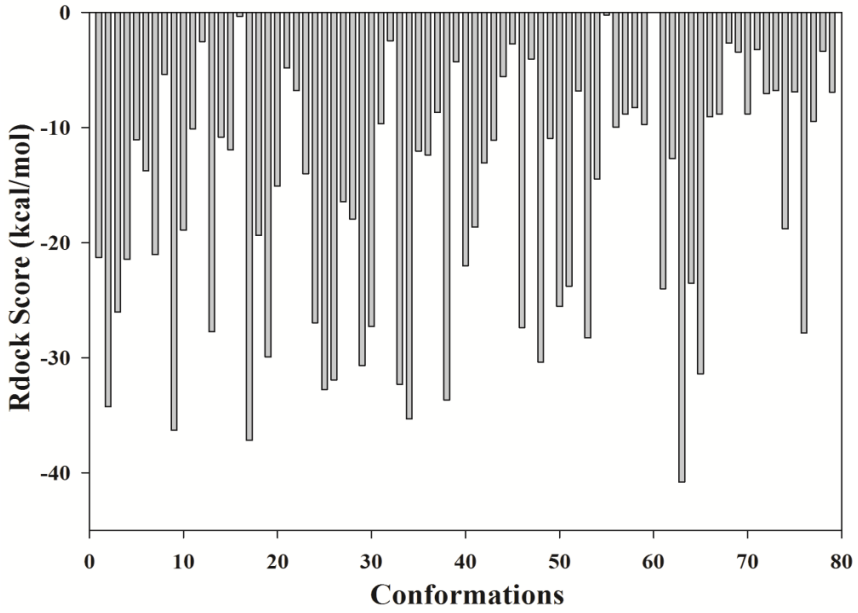

Figure 25: Comparison of $\Delta G_{binding}$ energy of different docking complexes between α/β tubulin and γ-tubulin calculated using Rdock

Molecular Dynamics Simulation

The selected complex was simulated in Gromacs (4.4) using Amber99SB force field for 10 ns in order to determine stability of the complex. An average structure was then obtained from the last 2 ns of MD trajectory. The average structure so obtained was then minimized and equilibrated in amber 11 using the parameters as described for γ-γ tubulin complex in chapter 1. The structure was then subjected to a 2ns MD simulation with a time step of 2 fs. A total of 2000 frames were generated.

Calculation of binding free energy between GCP4 and γ-tubulin

Binding free energy calculations were carried out using the conventional MM-PBSA and MM-GBSA approaches using Amber 11. A total of 200 snapshots were extracted, every 10 ps from the 2 ns of the MD trajectory. For each snapshot, the free energy was calculated for each molecular species (complex, protein and ligand). Conceptually the binding free energy can be calculated as :

$$\mathbf{\Delta G_{bind} = \Delta G_{complex} - [\Delta G_{rec} + \Delta G_{lig}]}$$

Per residue energy contribution

Energy decompostion method, implemented in Amber 11, was employed on the 200 frames extracted every 10 ps from 2 ns of simulation using the MM-GBSA method. The residues contributing more than 3 kcal/mol were considered very significant for the binding of GCP4 with γ-tubulin and these residues were designated as hotspot amino acids.

Computational Alanine Scanning Mutagenesis

To further study the energy contribution of these amino acids in the interaction of α/β tubulin and γ-tubulin, computational alanine scanning was performed. In this method an amino acid of interest is replaced with alanine and absolute binding free energy is recalculated. For our study we identified those amino acids which contributed significantly to the binding of α/β tubulin and γ-tubulin and were flanked by two or more polar amino acids. A total of 4 such segments were identified.

Experimental alanine scanning mutation and phenotypes

pALTER-EX1 vector (Promega, Madison, WI) was used to subclone *TUBG1* cDNA into the *NdeI* site downstream from the SP6 promoter to create pTWH101 as described by Hendrickson *et al*. [36]. Microtubule binding was evaluated with the mutated γ-tubulin proteins using tubulin binding assays.

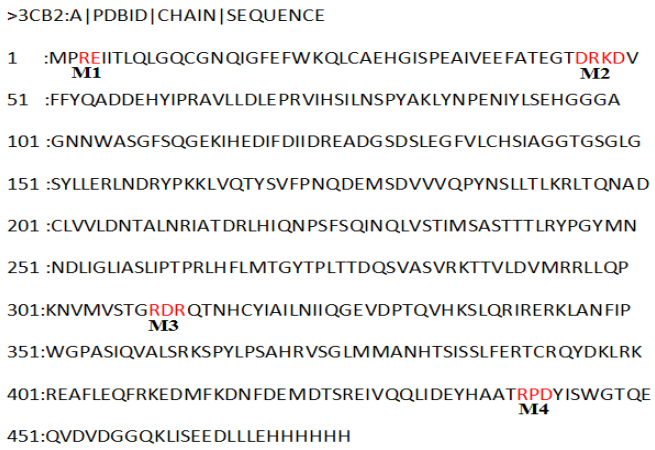

Figure 26: Amino acid stretches identified for alanine scanning mutagenesis. A total of seven stretched were identified on the basis of individual amino acid contribution and their participation interaction with α/β tubulin.

Results and discussions

A total of 2,000 conformations, categorized into 100 clusters, were generated after Zdock. On the basis of Zdock score and visual inspection to rule out unfavourable conformations, 132 conformations were selected for Rdock. A total of 79 conformations were found to have favourable Rdock score of which the conformation with least energy was obtained for molecular dynamics (Figure 25). The selected conformation was then simulated for 10 ns in Gromacs followed by a 2 ns simulation in Amber. A total of 200 frames were obtained, every 10 ps from 2ns MD trajectory. The calculation of binding free energy between the ligand and the complex of GCP4 and γ-tubulin was carried out using the MM-GBSA and MM-PBSA method. The results are summarized in table 10.

Table 10: Calculated binding free energy between α/β tubulin and γ-tubulin. Binding free energy calculated using MM-GBSA and MM-PBSA to ascertain the strength of interaction between α/β tubulin and γ-tubulin. The major energy components like van der Waals, electrostatic, polar solvation and non-polar solvation, contributing to the binding free energy were also estimated.

Contribution	Complex(kcal/mol)
ΔE_{INT}	0.00
ΔE_{VDW}	-284.61
ΔE_{ELE}	2027.56
ΔE_{GAS}	1742.95
ΔG_{PB}	-1821.50
ΔG_{SOL-NP}	-32.31
$\Delta G_{SOLV,PB}$	-1853.81
$\Delta G_{ELE,PB}$	206.06
$H_{TOT,PB}$	-110.86
G_{GB}	-1824.19
$G_{SOLV,GB}$	-1863.37
$G_{ELE\ GB}$	203.37
$H_{TOT,\ GB}$	-120.42

Per residue energy decomposition

Energy contribution of each residue in the interface between α/β tubulin and γ-tubulin was calculated using the MM-GBSA method to investigate the details of protein-protein interactions at the atomic level (Figure 27). We identified 15 hotspot amino acids that have the highest impact (per residue contribution > 2 kcal/mol) on the α/β tubulin and γ-tubulin interaction interface (Table 11).

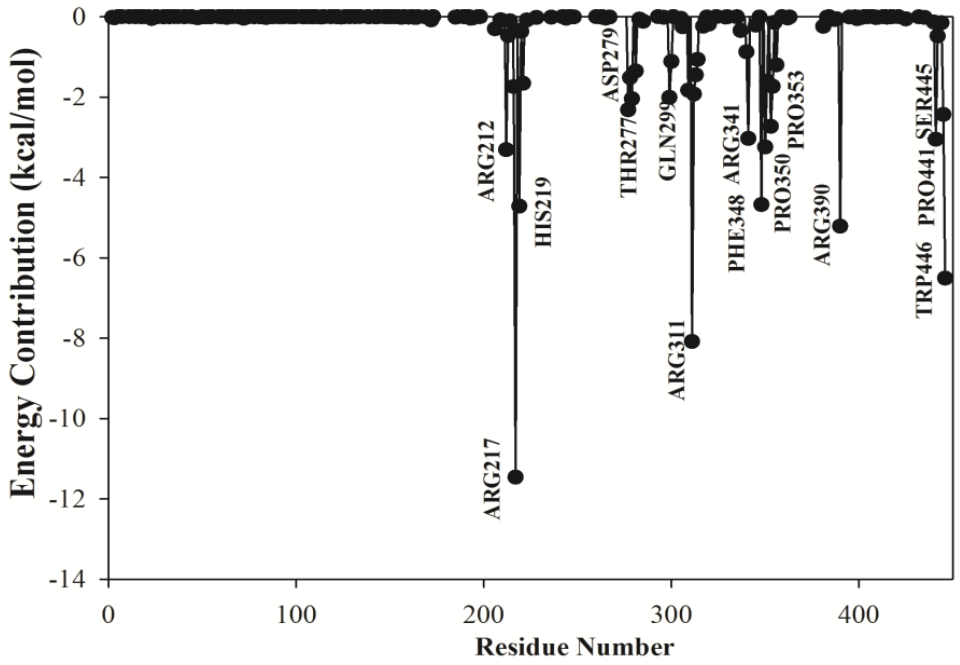

Figure 27: **Per residue free energy contribution of residues in the binding process of GCP4 and γ-tubulin.** Free energy contribution of each residue on the surface between α/β tubulin and γ-tubulin calculated based on MM-GBSA. Only the residues contributing free energy of >2 kcal/mol (designated as hotspot amino acids) are labelled in the figure.

Table 11. Decomposition of calculated $\Delta G_{bind,GB}$ (kcal/mol) on per residue basis into van der Waals, electrostatic, polar solvation and non-polar solvation energy components. A total of 15 residues with energy contribution of >2kcal/mol were obtained. The table also includes amino acids with energy contribution > 1kcal/mol.

Residue	$\Delta E_{i,vdw}$	$\Delta E_{i,ele}$	$\Delta G_{i,sol\ GB}$	$\Delta G_{i,sol-np}$	$\Delta H_{i,tot,GB}$
ARG211	-1.65	214.84	213.64	-0.46	-3.31
ASP215	-1.18	197.66	-197.92	-0.30	-1.74
ARG216	-1.23	250.77	240.94	-0.40	-11.46
HIE218	-5.96	-8.84	10.98	-0.90	-4.72
GLN220	-2.64	-8.92	10.72	-0.82	-1.66
THR276	-3.54	-1.29	2.94	-0.43	-2.32
THR277	-3.17	-1.70	3.92	-0.58	-1.52
ASP278	-1.81	191.34	-191.41	-0.16	-2.05
SER280	-0.52	-2.43	1.87	-0.28	-1.36
GLN298	-1.30	-9.85	9.39	-0.25	-2.01
PRO299	-1.87	-5.26	6.25	-0.24	-1.12
ARG308	-3.58	214.08	216.23	-0.41	-1.83
ARG310	-2.28	269.13	263.88	-0.56	-8.08
GLN311	-4.23	-2.91	5.94	-0.73	-1.93
THR312	-1.59	-0.89	1.25	-0.22	-1.45
ASN313	-0.55	-5.02	4.65	-0.14	-1.07
ARG340	-4.69	198.83	201.26	-0.77	-3.03
PHE347	-3.44	-1.30	0.44	-0.37	-4.68
PRO349	-3.43	-1.92	2.60	-0.48	-3.25
TRP350	-1.31	-1.89	1.67	-0.08	-1.61
PRO352	-2.98	-3.10	3.77	-0.43	-2.73
ALA353	-1.67	-3.49	3.71	-0.28	-1.74
ILE355	-1.17	-0.35	0.46	-0.14	-1.20
ARG389	-0.60	-217.28	212.97	-0.31	-5.22
PRO440	-3.45	-4.69	5.66	-0.58	-3.05
SER444	-1.90	-7.06	7.01	-0.48	-2.44
TRP445	-2.49	161.26	-164.68	-0.60	-6.51

Computational Alanine Scanning Mutagenesis

Each of the prepared mutant was MD simulated in Amber for 2 ns. This was followed by calculation of binding free energy (Table 12).

Table 12: Ensemble average of binding free energy (kcal/mol) of γ-γ tubulin complex calculated using the MM-GBSA and MM-PBSA methods in Amber

Complex	MM-GBSA (kcal/mol)	MM-PBSA (kcal/mol)
Wild Type	-120.49	-110.86
Mutant 1	-96.51	-65.25
Mutant 2	-90.90	-76.32
Mutant 3	-123.02	-119.95
Mutant 4	-79.24	-82.11

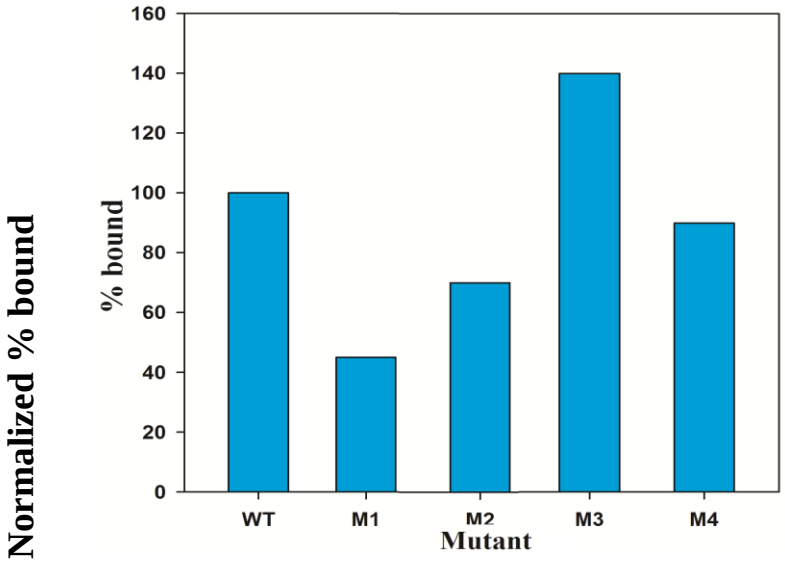

Figure 28: Normalized %bound of α/β tubulin with γ-tubulin.

Conclusion

The binding interface of γ-tubulin with α/β tubulin was identified using molecular modeling calculations. Residues playing crucial role in the interaction were also identified as hotspot amino acids. To further reinforce the hotspots, computational alanine scanning mutagenesis was performed. The results were further verified using the experimental alanine scanning mutagenesis. For three of the mutants- M1,M2 and M4 the binding affinity was lesser as compared to the wild type as observed after MM-GBSA analysis (Figure 28). Computationally identified interface was well verified by the experimental results.

References

1. StitesWE., "Protein-*protein interactions: interface structure, binding thermodynamics, and mutational analysis*", Chemical reviews 97 (5):1233-1250, 1997.
2. Rice LM., Montabana EA., Agard DA ., "*The lattice as allosteric effector: Structural studies of αβ-and γ-tubulin clarify the role of GTP in microtubule assembly*", Proceedings of the National Academy of Sciences 105 (14):5378-5383, 2008.
3. Wilson E.B., "*The cell in development and heredity*", 1928.
4. Li Q., Joshi HC., " *gamma-tubulin is a minus end-specific microtubule binding protein*", The Journal of cell biology 131 (1):207-214, 1995.
5. Oegema K., Wiese C., Martin OC., Milligan RA., Iwamatsu A., Mitchison TJ., Zheng Y., "*Characterization of two related Drosophila γ-tubulin complexes that differ in their ability to nucleate microtubules*", The Journal of cell biology 144 (4):721-733, 1999.
6. Zheng Y., Wong ML., Alberts B., Mitchison T., "*Nucleation of microtubule assembly by a gamma-tubulin-containing ring complex",* Nature 378 (6557):578-583, 1995.
7. Kollman, Justin M., et al. "*Microtubule nucleation by γ-tubulin complexes*."Nature Reviews Molecular Cell Biology 12.11 (2011): 709-721.
8. Oakley BR., Oakley CE., Yoon Y., Jung MK., "*γ-Tubulin is a component of the spindle pole body that is essential for microtubule function in Aspergillus nidulans*", Cell 61 (7):1289-1301, 1990.
9. Zheng Y., Jung MK., Oakley BR., " *γ-Tubulin is present in Drosophila melanogaster and Homo sapiens and is associated with the centrosome*", Cell 65 (5):817-823, 1991.

10. Stearns T., Evans L., Kirschner M., "*γ-Tubulin is a highly conserved component of the centrosome*", Cell 65 (5):825-836, 1991.
11. Horio T., Uzawa S., Jung MK., Oakley BR., Tanaka K., Yanagida M., " *The fission yeast gamma-tubulin is essential for mitosis and is localized at microtubule organizing centers*", Journal of cell science 99 (4):693-700, 1991.
12. Joshi HC., Palacios MJ., McNamara L., Cleveland DW., " *γ-Tubulin is a centrosomal protein required for cell cycle-dependent microtubule nucleation*", Nature 365:80-83, 1992.
13. Joshi HC., " *γ-Tubulin: The hub of cellular microtubule assemblies*", Bioessays 15 (10):637-643, 1993.
14. Oakley CE., Oakley BR., "*Identification of γ-tubulin, a new member of the tubulin superfamily encoded by mipA gene of Aspergillus nidulans*", Nature 338:662-664, 1989.
15. Raynaud-Messina B., Merdes A., "*g-Tubulin complexes and microtubule organization*",Curr Opin Cell Biol;19:24–30, 2007.
16. Niu Y, Liu T., Tse GM., Sun B., Niu R., Li HM., Wang H., Yang Y., Ye X., Wang Y., Yu Q., Zhang F., " *Increased expression of centrosomal a, g-tubulin in atypical ductal hyperplasia and carcinoma of the breast*", Cancer Sci;100:580–587, 2009.
17. Liu T., Niu Y., Yu Y., Liu Y., Zhang F., "*Increased g-tubulin expression and P16INK4A promoter methylation occur together in preinvasive lesions and carcinomas of the breast*" , Mar;20(3):441-8. doi: 10.1093/annonc/mdn651, 2009.
18. Montero-Conde C., Martı´n-Campos JM., Lerma E., Gimenez G., Martı´nez-Guitarte JL., Combalı´a N., Montaner D., Matı´as-Guiu X., Dopazo .J, de Leiva A., Robledo M., Mauricio D., " *Molecular profiling related to poor prognosis in thyroid carcinoma*", Combining gene expression data and biological information. Oncogene; 27:1554–1561, 2007.
19. Li Y., Hussain M., Sarkar SH., Eliason J., Li R., Sarkar FH., " *Gene expression profiling revealed novel mechanism of action of Taxotere and Furtulon in prostate cancer cells*", BMC Cancer;5:7, 2005.
20. Orsetti B., Nugoli M., Cervera N., Lasorsa L., Chuchana P., Ursule L., Nguyen C., Redon R., du Manoir S., Rodriguez C., Theillet C., " *Genomic and expression profiling of chromosome 17 in breast cancer reveals complex patterns of alterations and novel candidate genes*", Cancer Res;64:6453–6460, 2004.
21. Katsetos CD., Reddy G., Dra´berova´ E., S ˇ mejkalova´ B., Del Valle L., Ashraf Q., Tadevosyan A., Yelin K., Maraziotis T., Mishra OP., Mo¨rk S., Legido A., Nissanov J., Baas PW., de Chadare´vian JP., Dra´ber P., " *Altered cellular distribution and subcellular sorting of g-tubulin in diffuse astrocytic gliomas and human glioblastoma cell lines*", J Neuropathol Exp Neurol;65:465–477, 2006.
22. Cala O., Remy MH., Guillet V., Merdes A., Mourey L., Milon A., Czaplicki G., "*Virtual and biophysical screening targeting the γ-tubulin complex–a new target for the inhibition of microtubule nucleation*", PLoS One 2013 May 15;8(5):e63908. doi: 10.1371/journal.pone.0063908.
23. Aldaz, H., Rice, L.M., StearnsT., and Agard., D.A., "*Insights into microtubule nucleation from the crystal structure of human gamma-tubulin*", Nature;435, 523–527, 2005.
24. Hess B., Kutzner C., Van Der Spoel D., Lindahl E., "*GROMACS 4: Algorithms for highly efficient, load-balanced, and scalable molecular simulation*", Journal of chemical theory and computation 4 (3):435-447, 2008.
25. Laskowski RA., MacArthur MW., Moss DS., Thornton JM., "*PROCHECK: a program to check the stereochemical quality of protein structures*", Journal of applied crystallography 26 (2):283-291, 1993.
26. Ramachandran G., Ramakrishnan Ct., Sasisekharan V., "*Stereochemistry of polypeptide chain configurations*", Journal of molecular biology 7 (1):95-99, 1963.
27. Colovos C., Yeates TO., "*Verification of protein structures: patterns of nonbonded atomic interactions*", Protein Science 2 (9):1511-1519, 1993.

28. Eisenberg D., Lüthy R., Bowie JU., "*VERIFY3D: assessment of protein models with three-dimensional profiles*",Methods in enzymology 277:396, 1997.
29. Case DA., Cheatham TE., Darden T., Gohlke H., Luo R., Merz KM., Onufriev A., Simmerling C., Wang B., Woods RJ., "*The Amber biomolecular simulation programs*", Journal of computational chemistry 26 (16):1668-1688, 2005.
30. Pearlman DA., Case DA., Caldwell JW., Ross WS., Cheatham III TE., DeBolt S., Ferguson D., Seibel G., Kollman P., " *AMBER, a package of computer programs for applying molecular mechanics, normal mode analysis, molecular dynamics and free energy calculations to simulate the structural and energetic properties of molecules*", Computer Physics Communications, 91 (1):1-41, 1995.
31. Kollman PA., Massova I., Reyes C, Kuhn B., Huo S., Chong L., Lee M., Lee T., Duan Y., Wang W., "*Calculating structures and free energies of complex molecules: combining molecular mechanics and continuum models*", Accounts of chemical research 33 (12):889-897, 2000.
32. Massova I., Kollman PA., "*Combined molecular mechanical and continuum solvent approach (MM-PBSA/GBSA) to predict ligand binding*", Perspectives in Drug Discovery and Design 18 (1):113-135, 2000.
33. Kortemme T., Baker D., "*A simple physical model for binding energy hot spots in protein–protein complexes*", Proceedings of the National Academy of Sciences 99 (22):14116-14121, 2002.
34. Kortemme T., Kim DE., Baker D., "*Computational alanine scanning of protein-protein interfaces*", Science Signaling 2004 (219):pl2, 2004.
35. Liu H., Yao X., " *Molecular basis of the interaction for an essential subunit PA− PB1 in influenza virus RNA polymerase: insights from molecular dynamics simulation and free energy calculation*", Molecular pharmaceutics 7 (1):75-85, 2009.
36. Hendrickson TW., Yao J., Bhadury S., Corbett AH., Joshi HC., "*Conditional mutations in γ-tubulin reveal its involvement in chromosome segregation and cytokinesis*", Molecular biology of the cell 12 (8):2469-2481, 2001.
37. Maundrell K.,b nmt1 of fission yeast, " *A highly transcribed gene completely repressed by thiamine*", Journal of Biological Chemistry 265 (19):10857-10864
38. Maundrell K., "*Thiamine-repressible expression vectors pREP and pRIP for fission yeast*", Gene 123 (1):127-130, 1993.
39. Horio T, Oakley BR., "*Human gamma-tubulin functions in fission yeast*". The Journal of cell biology 126 (6):1465-1473, 1994.
40. Cornell WD, Cieplak P, Bayly CI, Gould IR, Merz KM, Ferguson DM, Spellmeyer DC, Fox T, Caldwell JW, Kollman PA. "*A second generation force field for the simulation of proteins, nucleic acids, and organic molecules*". Journal of the American Chemical Society117 (19):5179-5197, 1995.
41. Hornak V, Abel R, Okur A, Strockbine B, Roitberg A, Simmerling C. "*Comparison of multiple Amber force fields and development of improved protein backbone parameters*",Proteins: Structure, Function, and Bioinformatics 65 (3):712-725, 2006.
42. Lee C, Yang W, Parr RG. "*Development of the Colle-Salvetti correlation-energy formula into a functional of the electron density".* Phys Rev 1988;B 37:785-789.
43. Becke AD. "A new mixing of "*Hartree-Fock and local density-functional theories*". J ChemPhys 1993;98:1372-1377.
44. Binkley JS, Pople JA, Hehre WJ. "*Self-consistent molecular orbital methods. 21. Small split-valence basis sets for first-row elements."* J Am ChemSoc 1980;102:939-947.
45. Gordon MS, Binkley JS, Pople JA, Pietro WJ, Hehre WJ. "*Self-consistent molecular-orbital methods. 22. Small split-valence basis sets for second-row elements*." J Am ChemSoc 1982;104:2797-2803.
46. Pietro WJ, Francl MM, Hehre WJ, Defrees DJ, Pople JA, Binkley JS. "*Self-consistent molecular orbital methods. 24. Supplemented small split-valence basis sets for second-row elements".* J Am ChemSoc 1982;104:5039-5048.

47. Naik PK,Santoshi S, Rai A, Joshi HC. "*Molecular modelling and competition binding study of Br- Noscapine and colchicine provide insight into noscapinoid-tubulin binding site*". J. Mol. Graphics and Model;29: 947-955, 2011.
48. Halgren TA, Murphy RB, Friesner RA, Beard HS, Frye LL, Pollard WT, Banks JL. "*Glide: a new approach for rapid, accurate docking and scoring. 2. Enrichment factors in database screening*". J. Med. Chem;47: 1750-1759, 2004.
49. Friesner RA, Banks JL, Murphy RB, Halgren TA, Klicic JJ, Mainz DT, Repasky MP, Knoll EH, Shelley M, Perry JK, ShawDE, Francis P, Shenkin PS. *"Glide: a new approach for rapid, accurate docking and scoring. 1. method and assessment of docking accuracy*". J. Med. Chem;47: 1739–1749, 2004.
50. Wang J, Wang W, Kollman PA, Case DA. "*Automatic atom type and bond type perception in molecular mechanical calculations*". J Mol Graph Model;2:247–260. 2006
51. Jakalian A, Jack DB, Bayly CI. "*Fast, efficient generation of high-quality atomic charges . AM1-BCC model: I I .Parameterization and validation*". J Comput Chem;23:1623–1641, 2002.

LIST OF PUBLICATIONS

1. **Suri, Charu**, and Pradeep Kumar Naik (2012). To study the precise interaction of reduced and oxidized states of Neuroglobin with Ubc12 and Cop9 using molecular mechanics studies. *International Journal of Fundamental & Applied Sciences*. 1(4): 74-77.[ISSN: 2278-1404]

2. **Charu Suri,** Triscia W. Hendrickson, Harish C. Joshi, and Pradeep Kumar Naik (2014). "Molecular insight into γ–γ tubulin lateral interactions within the γ-tubulin ring complex (γ-TuRC)." *Journal of computer-aided molecular design*: DOI: 10.1007/s10822-014-9779-2 [ISSN: 0920-654X**, IF: 3.172]**

3. **Charu Suri,** Harish C. Joshi, and Pradeep Kumar Naik (2014). Molecular modelling reveals binding interface of γ-tubulin with GCP4 and interactions with noscapinoids. (Under review in journal of *PROTEINS: Structure, Function, and Bioinformatics* **IF**: **2.921**)

CONFERENCE PRESENTATIONS

1. **Charu Suri** and Pradeep K. Naik. Refinement of low resolution X-ray crystallographic protein structure utilizing molecular mechanics and molecular dynamics simulation techniques. **Presented** in International conference on "biotechnology advances :omics approaches and way forward (ICBA-2012)"organized by centre of biotechnology (supported by DST-FIST, govt. of India) Siksha 'o' Anusandhan University, Bhubaneswar 20 -22 December, 2012.)